

**UNIVERSITY OF SÃO PAULO
SÃO CARLOS SCHOOL OF ENGINEERING**

Edsson Frank Medina Vigoria

**A hybrid method (MVMO+TSM) for the parameter
estimation of one-axis generators model**

São Carlos

2023

Edsson Frank Medina Vigoria

**A hybrid method (MVMO+TSM) for the parameter
estimation of one-axis generators model**

Dissertation submitted to the São Carlos
School of Engineering of the University of
São Paulo in partial fulfillment of the require-
ments for the degree of Master of Science in
Electrical Engineering.

Area: Electrical Power Systems

Advisor: Prof. Dr. Elmer Pablo Tito Cari

**São Carlos
2023**

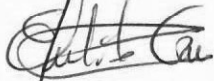
FOLHA DE JULGAMENTO

Candidato: Bacharel **EDSSON FRANK MEDINA VIGORIA**.

Título da dissertação: "Um método híbrido (MVMO+TSM) para a estimação de parâmetros do modelo de geradores de um eixo".

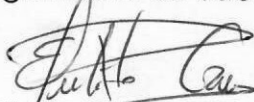
Data da defesa: 11/05/2023.

Comissão Julgadora

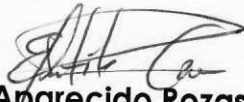


Prof. Dr. **Elmer Pablo Tito Cari**
(Orientador)

(Escola de Engenharia de São Carlos – EESC/USP)



Profa. Dra. **Tatiane Cristina da Costa Fernandes**
(Universidade Federal de São Carlos/UFSCar)



Prof. Dr. **Edson Aparecido Rozas Theodoro**
(Universidade Tecnológica Federal do Paraná/UTFPR)

Resultado

Aprovado

Aprovado

Aprovado

Coordenador do Programa de Pós-Graduação em Engenharia Elétrica:
Prof. Associado **Marcelo Andrade da Costa Vieira**

Presidente da Comissão de Pós-Graduação:
Prof. Titular **Carlos De Marqui Junior**

I dedicate this work with great love: to my parents Francisco and Gloria (who without them I would not be here), to my sister Rosa for their help in the most difficult times, to Carlos Triveño and his wife Marcia who are an inspiration for me and to all my family who has always been by my side.

The dedication put into this work in memory of Rony Aima Chaco.

ACKNOWLEDGEMENTS

I deeply appreciate:

- Professor Elmer Pablo Tito Cari for his excellent guidance and understanding during this work.
- Colleagues of the LACOSEP for their friendship.
- Professor Manuel Lau Pacheco for teaching, guidance and friendship in the area of electrical machines.
- All my friends for their good wishes.

RESUMO

VIGORIA, E. F. M. **Um método híbrido (MVMO+TSM) para a estimação de parâmetros do modelo de geradores de um eixo.** 2023. 91p. Dissertation (Master's degree) - São Carlos School of Engineering, University of São Paulo, São Carlos, 2023.

O conhecimento dos parâmetros do modelo transitório do gerador síncronos é fundamental para os estudos dinâmicos, o qual é usado para fazer planejamento e análises de segurança do sistema elétrico de energia. Normalmente, os parâmetros são determinados por meio de métodos offline (com o gerador desconectado da rede), porém, novas pesquisas utilizam métodos online (com o gerador conectado a rede) devido as vantagens para obter os valores dos parâmetros em diferentes condições de operação, com este propósito o método precisa ser confiável e robusto. Neste trabalho apresenta-se um método híbrido para estimar os parâmetros do modelo de um eixo do gerador síncrono com o propósito de fazer a estimação com medidas que são fácil obtenção e robusto em relação a convergência de parâmetros. Este método híbrido é composto por um método metaheurístico chamado Otimização de Mapeamento de Media-Variância (MVMO) e um método de programação não-linear chamado Sensibilidade de Trajetória (TSM). O método MVMO é utilizado para fornecer uma estimativa inicial inteligente para o segundo método (TSM), o qual será usado para encontrar o mínimo local, portanto, o método híbrido aproveita as vantagens do método metaheurístico e da programação não linear. O método é validado estimando os parâmetros de um gerador síncrono de 2 *kva* em um pequeno sistema de potência montado em laboratório com excelente resultados.

Palavras-chave: Gerador Síncrono, Estimação de Parâmetros, Método Híbrido, MVMO, Sensibilidade de Trajetória, Convergência.

ABSTRACT

VIGORIA, E. F. M. **A hybrid method (MVMO+TSM) for the parameter estimation of one-axis generators model.** 2023. 91p. Dissertation (Máster's Degree) - São Carlos School of Engineering, University of São Paulo, São Carlos, 2023.

The knowledge of parameters of transient model of the synchronous generator is fundamental for dynamic studies, which is used to make planning and analysis of security of the electrical energy system. Normally, the parameters are determined through offline methods (with the generator disconnected from the grid), however, new research uses online methods (with the generator connected to the grid) due to the advantages to obtain parameter values in different operation conditions, with this purpose the method needs to be reliable and robust. In this work, a hybrid method is presented to estimate the parameters of the one-axis model of the synchronous generator with the purpose of making the estimation with measures that are easy to obtain and robust in relation to the convergence of parameters. This hybrid method is composed of a metaheuristic method called Media-Variance Mapping Optimization (MVMO) and a non-linear programming method called Trajectory Sensitivity (TSM). The MVMO method is used to provide a smart initial guess for the second method (TSM), which will be used to find the local minimum, therefore, the hybrid method takes advantage of the metaheuristic method and non-linear programming. The method is validated by estimating the parameters of a 2 *kva* synchronous generator in a small power system assembled in the laboratory with satisfactory results.

Keywords: Synchronous generator, Parameter Estimation, Hybrid Method, MVMO, Trajectory Sensitivity, Convergence.

LIST OF FIGURES

| | |
|---|----|
| Figure 1 – Relation between reference system of the machine ($d - q$) and the grid ($I_m - R_e$) | 26 |
| Figure 2 – Identifiability analysis proposed in (LANDGRAF, 2022) | 32 |
| Figure 3 – Flowchart of estimation method | 33 |
| Figure 4 – Flowchart of hybrid method to parameter estimation | 35 |
| Figure 5 – Mean-variance mapping optimization | 37 |
| Figure 6 – Procedure, step by step, for MVMO | 38 |
| Figure 7 – New individual obtained from parent individual in offspring generator process | 39 |
| Figure 8 – Electric power system for testing the mechanical parameters | 41 |
| Figure 9 – Initial and final estimation process of the mechanical parameters with the hybrid method | 45 |
| Figure 10 – Electric Power System built for the obtaining of measurement data for electric parameters | 45 |
| Figure 11 – Outputs of EES after the parameter fitting of the Hybrid Method | 51 |
| Figure 12 – Outputs of EES for validation results provided by the Hybrid Method | 51 |
| Figure 13 – Mechanical Parameter Estimation GUI | 52 |
| Figure 14 – Mechanical Parameter Estimation GUI | 53 |
| Figure 15 – Results of the Mechanical Parameter Estimation GUI | 54 |
| Figure 16 – Results of the Mechanical Parameter Estimation GUI | 55 |
| Figure 17 – Results of the electrical Parameter Estimation GUI | 55 |
| Figure 18 – Schematic representation of a synchronous machine | 62 |
| Figure 19 – Representation of $dq0$ components of terminal voltage and current armature in relation to the synchronous reference | 76 |
| Figure 20 – Equivalent circuits of d-axis and q-axis in relation with the flows and currents | 78 |
| Figure 21 – Complete equivalent circuits of d-axis and q-axis | 79 |
| Figure 22 – Procedure step by step for MVMO | 87 |
| Figure 23 – Representation of the factor f_d | 88 |
| Figure 24 – Selection of the best individual. | 89 |
| Figure 25 – Gene of the parent replaced in the mapping function. | 89 |
| Figure 26 – Concentration around the mean value. | 90 |
| Figure 27 – New individual p_{new} obtained from p_{parent} remaining elements of p_i | 90 |
| Figure 28 – Population with the new individual without ranked. | 90 |
| Figure 29 – Population ranked from the best to the worst individuals including the new individual and discarding the worst one. | 91 |

LIST OF TABLES

| | |
|---|----|
| Table 1 – Nomenclature of different parameters of synchronous machine | 18 |
| Table 2 – Research works developed in LACOSEP for parameter estimation with hybrid method | 21 |
| Table 3 – Nomenclature for TSM and MVMO | 36 |
| Table 4 – Mechanical Parameters of Generator of 220 MVA obtained of (LAND- GRAF, 2014) used as benchmark | 42 |
| Table 5 – Results of MVMO for 10 individuals (Case 1) | 42 |
| Table 6 – Results of MVMO for 50 individuals (Case 2) | 43 |
| Table 7 – Results of TSM from initial guess with a difference ± 10 of the reference parameter | 43 |
| Table 8 – Results of TSM from initial guess with a difference ± 30 of the reference parameter | 43 |
| Table 9 – Hybrid method results | 44 |
| Table 10 – Information on disturbances data obtained from (CARI; LANDGRAF; ALBERTO, 2017) | 46 |
| Table 11 – Parameter of 2KVA Generator obtained from (LANDGRAF, 2022) and used as a benchmark | 46 |
| Table 12 – Parameter limits in p.u. for salient pole rotor used for MVMO | 46 |
| Table 13 – Results of MVMO for 10 individuals (Case 1) | 47 |
| Table 14 – Results of MVMO for 50 individuals (Case 2) | 48 |
| Table 15 – Results of TSM from initial guess with a difference ± 10 of the reference parameter value | 49 |
| Table 16 – Results of TSM from initial guess with a difference ± 30 of the reference parameter value | 49 |
| Table 17 – Convergence of TSM for different initial guesses from limits of Table 12 | 49 |
| Table 18 – Hybrid method results | 50 |
| Table 19 – Principal bases of magnitudes of the stator | 70 |
| Table 20 – Derived bases of magnitudes of the stator | 71 |
| Table 21 – Base magnitudes of the rotor | 72 |

CONTENTS

| | | |
|------------|---|-----------|
| 1 | INTRODUCTION | 17 |
| 1.1 | Motivation and Relevance | 17 |
| 1.2 | Parameter estimation method of synchronous generator | 17 |
| 1.3 | Research goals | 24 |
| 1.3.1 | General Goal | 24 |
| 1.3.2 | Specific Goals | 24 |
| 1.4 | Work organization | 25 |
| 2 | SYNCHRONOUS MACHINE MODELLING | 26 |
| 2.1 | Synchronous Generator Model for Estimation Purpose | 26 |
| 2.1.1 | Two-axis transient model | 26 |
| 2.1.2 | Two-axis transient model with estimation purpose | 27 |
| 2.1.3 | Improved model for the estimation of the one-axis model | 28 |
| 2.1.4 | Improved model to estimate the mechanical parameters of synchronous generator | 29 |
| 2.1.5 | Improved model to estimate the electric parameters of one-axis model | 30 |
| 3 | IDENTIFIABILITY AND PARAMETER ESTIMATION PROCESS | 32 |
| 3.1 | Estimation process | 33 |
| 3.2 | Hybrid Estimation Method | 34 |
| 3.2.1 | Mean-Variance Mapping Optimization Method (MVMO) | 37 |
| 3.2.2 | Trajectory Sensitivity Method | 39 |
| 4 | APPLICATION AND RESULTS | 41 |
| 4.1 | Mechanical Parameter Estimation | 41 |
| 4.1.1 | Benchmark for mechanical parameter estimation | 42 |
| 4.1.2 | Estimation of mechanical parameters with MVMO | 42 |
| 4.1.3 | Estimation of mechanical parameters with TSM | 43 |
| 4.1.4 | Results of Hybrid Method | 43 |
| 4.2 | Electric Parameter Estimation | 45 |
| 4.2.1 | Benchmark for parameter and optimal time period | 46 |
| 4.2.2 | Parameter Limits for the generator | 46 |
| 4.2.3 | Procedure for electric Parameter Estimation | 47 |
| 4.2.3.1 | Parameter Estimation by MVMO | 47 |
| 4.2.3.2 | Results of TSM | 48 |
| 4.2.3.3 | Results of Hybrid Method | 49 |

| | | |
|----------|--|-----------|
| 4.2.3.4 | Validation results | 51 |
| 5 | SOFTWARE FOR PARAMETER ESTIMATION OF SYNCHRONOUS GENERATOR - GENVALIDA 1.0. | 52 |
| 5.1 | Initial screen | 52 |
| 5.2 | Mechanical Parameters GUI | 53 |
| 5.3 | Electric Parameters GUI | 54 |
| 6 | CONCLUSIONS | 56 |
| 6.1 | Ongoing research | 56 |
| 6.2 | Published works | 56 |
| | BIBLIOGRAPHY | 57 |
| | ANNEX | 61 |
| | ANNEX A – GENERAL MODEL OF THE SYNCHRONOUS GENERATOR | 62 |
| | ANNEX B – MVMO ALGORITHM INFORMATION | 86 |

1 INTRODUCTION

1.1 Motivation and Relevance

Nowadays an important tool in the stability and planning studies of the Electric Energy System (EES) is the evaluation of the dynamic response during a disturbance. Therefore, the precise knowledge of the parameters of synchronous generators is very important in the specialized programs used in the electric sector, with the purpose to obtain simulations that show the dynamic behavior of EES. When the parameters are not estimated accurately, simulations cannot show the real behavior of the system, or in the worst case, the EES could operate in an insecure power margin that could lead to a system collapse (KOSTEREV N. D.;TAYLOR, 1999). On the other hand, the accurate knowledge of the parameters' values supports engineering in the determination of the correct power margin. Among the different components of the EES (synchronous generator, load models, wind turbine, etc), the synchronous generator model is one of the most important. Usually, the synchronous generator parameters are provided by manufacturers by off-line tests (Generator disconnect from the grid). However, those parameters change when the generator is in operation due to some parameters are subject to the saturation effect (LANDGRAF, 2014). In another case, when the information about generator parameters was lost, those values are obtained by other generators with similar characteristics.

1.2 Parameter estimation method of synchronous generator

For the aforementioned reasons, many studies about the estimation of synchronous generator parameters were proposed over time. The methods can be divided into two groups. First, is the "Offline method" with the generator disconnected from the grid. Those methods were standardized by the Institute of Electrical and Electronics Engineers (IEEE) (IEEE, 2018), (IEE, 2020). Such method has the disadvantage of disconnection the generator of the grid, which produces economic losses or is used only during the maintenance period. Second is the "Online method", which does not require the disconnection of the generator from the grid. The parameter values can be obtained in different operation conditions, both in stationary and transient conditions (HEYDT et al., 2005). For this reason, this kind of method to identify the parameters has become more attractive (BURTH; VERGHESE; VELEZ-REYES, 1999), (LANDGRAF, 2014), (ZAKER et al., 2015), (LANDGRAF; CARI; ALBERTO, 2022). Recent approaches for parameter estimation of the generator using phasor measurements signals are based on the Phasor Measurement Units (PMU) can be found in (LAVERTY et al., 2013), (ZIMMER; DECKER; SILVA, 2018), (GONZÁLEZ-CAGIGAL; ROSENDO-MACÍAS; GÓMEZ-EXPÓSITO, 2019).

The number of parameters to be estimated will depend on the level of detail of the model, as can be seen in Table 1.

Table 1 – Nomenclature of different parameters of synchronous machine

| Parameter | Name | Model |
|------------|---|---------------|
| E'_d | d- and q-axis transient voltages | Transient |
| E'_{q0} | Initial condition on unmeasured state E'_q (p.u) | Transient |
| E_{fd} | Field voltage (p.u) | Transient |
| I_d, I_q | d- and q-axis stator currents (p.u) | Transient |
| K_e | Field voltage required for the production of rated air-gap line voltage (volts) | Transient |
| P_e, Q_e | Electric and Reactive Power (p.u) | Transient |
| P_m | Mechanical Power (p.u) | Transient |
| T'_{d0} | d-axis open circuit transient time constant (s) | Transient |
| V_d, V_q | d- and q-axis stator voltage (p.u) | Transient |
| V_{fd} | Actual field voltage (volts) | Transient |
| V_t, I_t | Stator terminal voltage and current | Transient |
| x'_d | d-axis transient reactance (p.u) | Transient |
| x_d, x_q | d- and q-axis synchronous reactance | Transient |
| β | Load angle (rad) | Transient |
| α | Rotor angle (rad/s) | Transient |
| ω | Rotor frequency (rad/s) | Transient |
| ω_s | Synchronous frequency (rad/s) | Transient |
| θ | Terminal Voltage phase angle (rad/s) | Transient |
| D | Damping coefficient (p.u) | Transient |
| H | Inertia constant (p.u) | Transient |
| T'_{kd} | Direct-axis damper leakage time constant (p.u) | Transient |
| T''_d | Time sub-transient constant of open circuit in the direct axis | Sub-transient |
| T_o | Armature winding time constant | Transient |
| R_s | Stator Resistance | Transient |
| L_d, L_q | d- and q-axis inductances | Transient |

Regarding the algorithm using parameter estimation methods, metaheuristic methods, (ERLICH; VENAYAGAMOORTHY; WORAWAT, 2010), (KOOSHKBAGHI; MARQUEZ; XU, 2019) have been proposed in the scientific community. It allows the estimation of the parameter within a large parameter search region; however, it could take a lot of time, especially when the estimation is near the parameter value (BLUM; ROLI, 2003), (ERLICH; VENAYAGAMOORTHY; WORAWAT, 2010), (GUNEN et al., 2020).

An example of a metaheuristic method is the Adaptive Black Widow Optimization (ABWO) used in (MICEV et al., 2020) for the identification of synchronous generator parameters based on a sudden short circuit test. The field current waveform is used to obtain the transient parameters. The research considers a simple model with one damper winding on each axis, where a sudden three-phase short circuit of the generator is carried out in order to obtain an experimental waveform of the field current. Consequently the

parameters " $x_d, x'_d, (T'_d), (T'_{kd}), (T''_d)$, and (T_a) " are extracted using "ABWO", which is based on adaptive change of the parameters of the algorithm what provides an increase in the convergence speed and accuracy in the results.

On the other hand, nonlinear programming methods allow finding the local minimum faster. However, they are dependent on the initial condition. Some examples of this kind of methods are the Kalman filter, which is used through a variant of this method (Unscented Kalman Filter) in (GONZÁLEZ-CAGIGAL; ROSENDO-MACÍAS; GÓMEZ-EXPÓSITO, 2019) to estimate 16 parameters of generic equivalent of synchronous generator composed by Speed governor, Automatic voltage regulator, Power system stabilizer, Synchronous generator, where the parameters are:

| Speed Governor | Automatic Voltage Regulator | Power system Stabilizer | Synchronous Generator |
|---|--|-----------------------------|---|
| Governor droop (R) | Controller Time Constant (T_{avr}) | PSS Time Constant (T_W) | Damping Coefficient (D) |
| Primary Control Time Constant (T_r) | Exciter Time Constant (T_e) | PSS Gain (K_W) | Inertia Constant (H) |
| Secondary Control Gain (K_d) | AVR Gain (K_0) | | q and d axis synchronous reactances (x_q), (x_d) |
| | | | q and d transient reactances (x'_q), (x'_d) |
| | | | q and d axis transient time constant (T'_{q0}), (T'_{d0}) |

The before-mentioned research uses the next measurement data "Voltage at the generator bus (V), Phase angle (θ), stator current (I), Rotor angle speed (ω), Electric Power (P_e)". Therefore, the method is dependent on PMU to execute the estimation.

Another method used in (CHOI et al., 2019) is the Recursive Least-Squares (RLS) to estimate in real time the parameters of the permanent magnet synchronous motor (PMSM) based on the stator current ripple model. The RLS algorithm allows a complete online estimation of the parameters. Where three electric parameters of the Permanent Magnet Synchronous Rotor are estimated " R_s, L_d , and L_q ".

In the same way, (ZHU; LIANG; LIU, 2021) used the Multistep estimation method where the electric parameters are estimated in three steps, first the R_s and distorted voltage (V_{dead}) are estimated by injection at standstill, after rotor flux linkage (ψ_{pm}), inductances in L_d, L_q and it is estimated online by fixing rotor flux linkage (ψ_{pm}) at the second step. However, estimation is very dependent on the sensors and inverter. If it has bad conditioning of those measurements it can not provide good results.

Finally, the Laboratory of Computing Assessment in Electric Power Systems (LACOSEP) of EESC/USP has been developing the same application of the trajectory sensitivity method (TSM), Mean-Variance Mapping Optimization Method (MVMO), and hybrid method (MVMO + TSM) to determine the parameters of different elements in the electric power system as can be seen in table 2.

Table 2 – Research works developed in LACOSEP for parameter estimation with hybrid method

| Author | Year | Work | Work's name | Method | Abstract |
|---|------|----------------------------------|--|--------|---|
| Cari, E. P. T.; Alberto, L. F. C. | 2005 | Master Dissertation | Methodology for the Parameter Estimation of Synchronous Generator and Excitation System | TSM | In this work is proposed a methodology for online estimation the parameters of synchronous generator based on the trajectory sensitivity technique. |
| Cari, E. P. T.; Alberto, L. F. C. | 2009 | Thesis | Methodology for Nonlinear Parameter Estimation with Application to Synchronous Generators | TSM | In this work is developed a new methodology for estimation of nonlinear dynamic systems based on the trajectory sensitivity, also is developed the independent estimation of mechanical and electric parameters through readily available measures. |
| Beordo, L. | 2014 | Final report of undergraduate | Experimental determination of the parameters of a synchronous generator test (off-line) and via trajectory sensitivity analysis technique (online) | TSM | In this work is developed a comparison between conventional techniques (off-line test) with a technique based on trajectory sensitivity analysis to estimate parameters of the synchronous generator (on-line test). |
| Landgraf, T. G.; Cari, E. P. T. | 2014 | Master Dissertation | Modeling and Estimation of Parameters of Synchronous Generators by means of Trajectory Sensitivity Analysis | TSM | In this work is developed a new simplify model used for parameter estimation of synchronous generator, which is modified of two-axis model, where the field current is used as an input. |
| Cari, E.; Landgraf, T.; Alberto, L. F. C; | 2016 | Paper | A constrained minimization approach for the estimation of parameters of transient generator models | TSM | This paper proposes a parameter estimation of the synchronous generator, where its solution is based on a minimization of the norm of algebraic equations of the transient model of the synchronous generator subject to differential equations constraints. |

| Author | Year | Work | Work's name | Method | Abstract |
|---|------|------------------------|--|------------|--|
| Cari, E. P. T.; Alberto, L. F. C. | 2017 | Article | Parameter estimation of load models using a hybrid heuristic and nonlinear approach | TSM | Hybrid Estimation of load models using evolutionary method (MVMO) plus nonlinear programming (TSM). |
| Ecyo, F. R. C.; Cari, E. P. T.; Erlich, I.; Fedaku, S. | 2018 | Paper | Online Parameter Estimation of a Transient Induction Generator Model based on Hybrid Method | TSM + MVMO | This works proposes a hybrid method (MVMO+TSM) for online parameter estimation of induction generator transient models using measurements commonly available in practice. |
| Fioravante, B. S. | 2019 | Final report of course | Software development for parameters of the electric machine by the short circuit test | TSM | The parameters of the synchronous generator were estimated through the short-circuit test, where the sensitivity method was used to obtain the parameters. |
| Moura, P. F. | 2019 | Final report of course | Software development for estimation of parameters of the electric machine by the load rejection test | TSM | The parameters of the synchronous generator for estimation of nonlinear dynamic systems were estimated through the load rejection test, where the sensitivity method was used to obtain the parameters. |
| Lemes, F. R.; Gomes, G. J. N.; Cari, E. P. T. | 2020 | Paper | Load Model Identification through a Hybrid Approach | TSM + MVMO | This works proposes a hybrid method (MVMO+TSM) to estimate the parameters of load model from online measurements obtained from tap changes of transformers |
| Gomes, G. J. N.; Cari, E. P. T. | 2020 | Master Dissertation | Parameter Estimation of Wind Power Plant Equivalent Model through a Hybrid Method | TSM + MVMO | This works proposes a hybrid estimation method to estimate parameters of a wind power plant generic model. At first, is used an evolutionary method (MVMO). When the parameters are close enough to their real values, nonlinear programming (TSM) is applied to improve the results and optimize solution. Combining both methods results in a fast and robust estimation approach. |

| Author | Year | Work | Work's name | Method | Abstract |
|--|------|-------|--|------------|---|
| Landgraf, T.G.; Cari, E. P. T; Alberto, L. F. C. | 2022 | Paper | An Analysis of Structural and Practical Identifiability Applied to a Transient Generator Model | TSM | This work addresses issues of the structural and practical identifiability of a transient model of a synchronous generator, also is selected an optimal time window of measurement data for improving the accuracy of the estimated parameters. |
| Viguria, M. E. F; Cari, E. P. T. | 2023 | paper | Hybrid Estimation of Mechanical Parameters of Synchronous Generator | TSM + MVMO | This works developed a hybrid estimation method, which uses an evolutionary method (MVMO) to has a large parameter search region to find a smart initial guess, which is close to the true value to estimate the mechanical parameters of synchronous generator through nonlinear programming method (TSM). |

1.3 Research goals

1.3.1 General Goal

Develop a robust and reliable estimation process for the transient synchronous generator model based on a hybrid method composed of the MVMO and TSM algorithms.

1.3.2 Specific Goals

- a. Develop the MVMO and the TSM algorithms to estimate the parameters of the transient generator model.
- b. Make independent the initial guess for TSM through an intelligent initial guess provided by MVMO.
- c. Robustness in relation to the convergence of parameters.
- d. Combine the benefits of both methods to provide a robust and reliable estimation process.
- e. Online parameter estimation from easily accessible measurement.
- f. Development of a synchronous generator parameter estimation software.

This thesis is the continuation of previous works ([FARIAS et al., 2018](#)), and ([LANDGRAF, 2022](#)) in which the hybrid method was applied to the induction generator model and an identifiability analysis was conducted for the synchronous generator model, respectively.

1.4 Work organization

The text is organized as follows:

- Chapter 2 shows the models of the synchronous generator with estimation purpose, which is divided in mechanical and electric parameters, as well as their variables, inputs, outputs, and parameters. Initially is shown the original model of the synchronous generator, and consequently, is shown the model of electric parameters for the one-axis model (salient pole rotor) with estimation purposes.
- Chapter 3 shows the hybrid estimation procedure, which contains how the MVMO and TSM algorithm works.
- Chapter 4 presents the results of the hybrid estimation, which contains the estimation of the mechanical and electric parameters, and the validation results.
- Chapter 5 shows the software developed for the one-axis generator model with a GUI interface.
- Chapter 6 Present the conclusion and ongoing research.
- Annex A shows the development of the principal original model of the synchronous generator used in electric power system studies. As well as is shown the bases adopted for the magnitudes of the system per unit and the equivalent circuits.

2 SYNCHRONOUS MACHINE MODELLING

The equations of the transient model of the synchronous generator (KUNDUR, 1994), (KIMBARK, 1995), (ANDERSON; FOUAD, 2008) were developed in detail in Annex A. Meantime, with parameter estimation purposes are necessary some modifications in the model are to facilitate the application in real cases. These modifications are based on the research work (LANDGRAF, 2022) and will be rewritten and presented in the next sections.

2.1 Synchronous Generator Model for Estimation Purpose

In (CARI, 2009) was developed an improved transient generator model for parameter estimation purposes from the traditional transient generator model (A.137)-(A.142). The advantages of the model are to diminish the number of parameters to be estimated and to use the measurements that can be obtained easily in the real system. Subsequently, in (LANDGRAF, 2022) was unwrapped an analysis of the structural and practical identifiability of the one-axis transient generator model for the selected parameter vector, states, algebraic variables, inputs, and outputs to ensure the estimation.

2.1.1 Two-axis transient model

In (CARI, 2005) a set of variables of input, output, and parameters were proposed for the transient synchronous generator model. Consequently, this model uses a special reference system as shown in Figure 1.

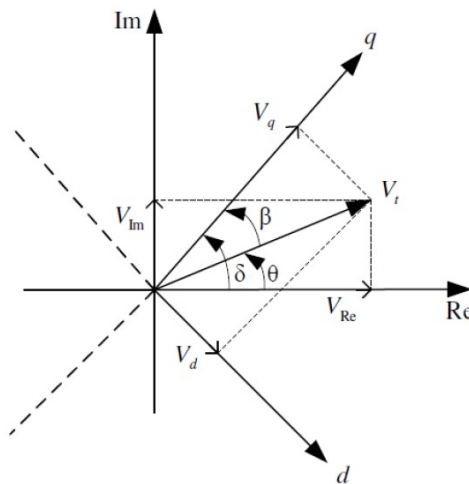


Figure 1 – Relation between reference system of the machine ($d-q$) and the grid ($I_m - R_e$)

Source: (LANDGRAF, 2022)

Two references are used to model the EES, the synchronous machine is modeled in the “ $d - q$ ” reference which is located in the rotor. One of the two axes is aligned with the magnetic axis of the field winding, which is known as the “direct axis”, and another axis is located 90° backward in relation to field winding, which is known as the “quadrature axis”. The EES is modeled in the $I_m - R_e$ (Synchronous reference), with the R_e axis 90° backward to the I_m axis, δ and θ are the angles of the quadrature axis and the terminal voltage, respectively. To simplify the analyses the reference voltage V_{Re} coincides with the R_e axis (LANDGRAF, 2022).

The differential equations that describe the transient model of the synchronous generator are (CARI, 2005):

$$\dot{\delta} = \omega \quad (2.1)$$

$$\dot{\omega} = \frac{\omega_s}{2H} \left(P_m - E'_q I_q - E'_d I_d - (x'_d - x'_q) I_d I_q - \frac{D}{\omega_s} \omega \right) \quad (2.2)$$

$$\dot{E}'_q = \frac{1}{T'_{d0}} \left(E_{fd} - E'_q + (x_d + x'_d) I_d \right) \quad (2.3)$$

$$\dot{E}'_d = \frac{1}{T'_{q0}} \left(-E'_d - (x_q + x'_q) I_q \right) \quad (2.4)$$

$$I_d = \frac{E_b \cos(\delta) + E'_q}{x'_d + Z_I} \quad (2.5)$$

$$I_q = \frac{E_b \sin(\delta) + E'_d}{x'_q + Z_I} \quad (2.6)$$

For this model, the features are:

| | |
|------------------|--|
| States: | $x = [\delta, \omega, E'_q, E'_d]$ |
| Parameters: | $p = [x_d, x'_d, T'_{d0}, x_q, x'_q, T'_{q0}]^T$ |
| Constants: | $c = [D, H, Z_I, E_b, \omega_s]$ |
| Input variables: | $u = [E_{fd}, P_m]$ |
| Output variable: | $y = [\delta, \omega]$ |

2.1.2 Two-axis transient model with estimation purpose

The transient model of the two-axis generator model is given by:

$$\dot{\delta} = \omega - \omega_s \quad (2.7)$$

$$\dot{\omega} = \frac{\omega_s}{2H} \left(P_m - E'_q I_q - E'_d I_d - (x'_q - x'_d) I_d I_q - D(\omega - \omega_s) \right) \quad (2.8)$$

$$\dot{E}'_q = \frac{1}{T'_{d0}} \left(-E'_q - (x_d - x'_d) I_d + E_{fd} \right) \quad (2.9)$$

$$\dot{E}'_d = \frac{1}{T'_{q0}} \left(-E'_d + (x_q - x'_q) I_q \right) \quad (2.10)$$

Where the algebraic equations of the stator are:

$$E'd - V_t \sin(\delta - \theta) + x'_q I_q = 0 \quad (2.11)$$

$$E'q - V_t \cos(\delta - \theta) - x'_d I_d = 0 \quad (2.12)$$

This model is obtained by neglecting the fast dynamics of the damper windings, time constants, sub-transient reactances, stator resistance, and saturation effect.

Figure 1 shows the coordinate references of the synchronous generator (d, q) and the grid (I_m, R_e). V_t denotes the magnitude of the generator terminal voltage and the rotor angle (δ) and the terminal voltage phase angle (θ) are measured in relation to the grid reference. The load angle (β) is the angular difference between (δ and θ).

The features of the model are:

$$\begin{aligned} \text{States:} & \quad x = [\delta, \omega, E'_q, E'_d] \\ \text{Parameters:} & \quad p = [H, D, x_d, x_q, x'_d, x'_q, T'_{d0}, T'_{q0}] \\ \text{Input variables:} & \quad u = [E_{fd}, P_m, V_t, \theta] \end{aligned}$$

2.1.3 Improved model for the estimation of the one-axis model

In this model, there is no damper winding on the q-axis to represent the eddy currents in the rotor body, therefore, $x'_q = X_q$ and $T'_{q0} = 0$, consequently, $E'_d = 0$. This model is similar to the two-axis model of subsection 2.1.2 except that the equation (2.10) is eliminated from the set of equations (2.7)-(2.10).

The original one-axis transient model of the synchronous generator is given by:

$$\dot{\delta} = \omega - \omega_s \quad (2.13)$$

$$\dot{\omega} = \frac{\omega_s}{2H} (P_m - E'_q - (x_q - x'_d)I_d I_q - D(\omega - \omega_s)) \quad (2.14)$$

$$\dot{E}'_q = \frac{1}{T'_{d0}} (-E'_q - (x_d - x'_d)I_d + E_{fd}) \quad (2.15)$$

where the stator algebraic equations are

$$V_t \sin(\delta - \theta) - x_q I_q = 0 \quad (2.16)$$

$$E'_q - V_t \cos(\delta - \theta) - x'_d I_d = 0 \quad (2.17)$$

Input E_{fd} in (p.u) is the field voltage in the base system related to actual field voltage V_{fd} (in volts) by

$$E_{fd} = \frac{V_{fd}}{K_e} \quad (2.18)$$

where K_e is a new parameter related to the field voltage [volts] required for the production of rated air-gap line voltage (KUNDUR, 1994).

The model is obtained neglecting the dynamics of damper windings, sub-transient time constants, reactances, and stator resistance (LANDGRAF, 2022).

The original one-axis model (2.13)-(2.18) uses the reference of Figure 1, has nine parameters and depends on the θ angle as input, which is difficult to measure in practice, therefore, has the following features:

$$\begin{aligned} \text{Parameters:} & \quad p = [H, D, x_d, x_q, x'_d, T'_{d0}, E'_{q0}, \delta_0, K_e] \\ \text{State variables:} & \quad x = [\delta, \omega, E'_q] \\ \text{Input variables:} & \quad u = [V_{fd}, P_m, V_t, \theta] \\ \text{Output variable:} & \quad y = [\omega] \end{aligned}$$

The system (2.13)-(2.18) is decoupled into mechanical, and electric models for improving the estimation. Such a decomposition reduces the number of parameters to be estimated simultaneously since the mechanical part becomes independent of the electric one. For both models, now, one has:

2.1.4 Improved model to estimate the mechanical parameters of synchronous generator

In (CARI, 2009) was proposed a methodology where is resolved this intrinsic problem and decreased the number of parameters to estimate. For this purpose, the model is decoupled into two independent parts, the mechanical parameters, and the electric parameters.

Considering the equations expressed in the sub-section A and substituting $P_e = E'_q I_q + E'_d I_d + (x'_d - x'_q) I_d I_q$ is possible to get the model of the mechanical parameters of synchronous generator:

$$\begin{aligned} \dot{\omega} &= \frac{\omega_0}{2H} \left[P_m - P_e - \frac{D}{\omega_0} \omega \right] \\ y &= [\omega] \end{aligned} \tag{2.19}$$

- P_m : Mechanical power can be obtained from the stable state as $P_m = P_{e0}$ and is regarded as constant during the transient period;
- P_e : Electric power, which is obtained through the measurements of the three-phase voltages and currents;
- ω_0 : Synchronous speed, where $\omega_0 = \frac{2}{np} \omega_e$ with $\omega_e = 2\pi f$, np is the number of poles of the machine and f is the frequency in Hz (In Brazil $f = 60$ Hz);
- D : Damping coefficient;
- H : Inertia constant;

Model 2.13 is completely decoupled of the electric variables and parameters, where their variables are:

$$\begin{aligned}
\text{Parameters:} & \quad p = [H, D]^T \\
\text{Constants:} & \quad c = [P_m, f, np]^T \\
\text{Input variables:} & \quad u = [P_e] \\
\text{Output variable:} & \quad y = [\omega]
\end{aligned}$$

2.1.5 Improved model to estimate the electric parameters of one-axis model

The next step is the implementation of the model to estimate the electric parameters of the synchronous generator, considering the equations developed in sub-section A, it is possible to get the model of the electric parameters of the synchronous generator.

The electric model is given by equation (2.15) and algebraic equations (2.16)-(2.17), which are functions of $(E'_q, \delta, V_t, \theta)$. However, angle (δ) from (2.13) was eliminated in the decoupling process and a current balance equation was added to the model for obtaining the load angle, β , instead of using " $\delta - \theta$ " in (2.16)-(2.17):

$$\dot{E}'_q = \frac{1}{T'_{d0}} \left(-E'_q - (x_d - x'_d)I_d + E_{fd} \right) \quad (2.20)$$

$$0 = I_t^2 - I_d^2 - I_q^2 \quad (2.21)$$

where:

$$I_q = \frac{V_t \sin(\beta)}{x_q} \quad (2.22)$$

$$I_d = \frac{E'_q - V_t \cos(\beta)}{x'_d} \quad (2.23)$$

The output of the models is the active and reactive power obtained from three-phase voltages and currents of the generator:

$$P_e = E'_q I_q + (x_q - x'_d) I_d I_q \quad (2.24)$$

$$Q_e = E'_q I_d - (x'_d I_d^2) - x_q I_q^2 \quad (2.25)$$

Finally, substituting I_d and I_q and E_{fd} , in (2.20)-(2.21) and (2.24)-(2.25), the electrical model is obtained by

$$\dot{E}'_q = \frac{1}{T'_{d0} x'_d} \left(-x_d E'_q + (x_d - x'_d) V_t \cos(\beta) + \frac{x'_d}{K_e} V_{fd} \right) \quad (2.26)$$

$$0 = I_t^2 - \frac{E_q'^2 - 2E'_q V_t \cos(\beta) + V_t^2 \cos^2(\beta)}{x_d'^2} - \frac{V_t^2 \sin^2(\beta)}{x_q^2} \quad (2.27)$$

$$P_e = \frac{E'_q V_t \sin(\beta)}{x'_d} + \left(\frac{1}{x_q} - \frac{1}{x'_d} \right) \sin(\beta) \cos(\beta) V_t^2 \quad (2.28)$$

$$Q_e = \frac{E'_q V_t \cos(\beta)}{x'_d} - \left(\frac{\sin^2(\beta)}{x_q} + \frac{\cos^2(\beta)}{x'_d} \right) V_t^2 \quad (2.29)$$

The feature for parameter estimation purposes for the model (2.26)-(2.29) are

$$\begin{aligned}
 \text{Parameters:} & \quad p = [x_d, x'_d, T'_{d0}, x'_q, K_e, E'_{q0}] \\
 \text{State variables:} & \quad x = [E'_q] \\
 \text{Algebraic variables:} & \quad x = [\beta] \\
 \text{Input variables:} & \quad u = [I_t, V_t, V_{fd}] \\
 \text{Output variables:} & \quad y = [P_e, Q_e]
 \end{aligned}$$

As addressed elsewhere, only easily obtainable measures are required for the model. Load angle (β) is extracted in each iteration through the balance current equation (2.27). Another piece of information is that the initial condition of state variable E'_{q0} is considered an unknown parameter. More information about the model can be found in (LANDGRAF; CARI; ALBERTO, 2022).

3 IDENTIFIABILITY AND PARAMETER ESTIMATION PROCESS

The relation between the outputs and inputs of the model left not all parameters can be estimated. Thus, the model identifiability problem is defined in two steps: structural identifiability and practical identifiability, as can be seen in Figure 2.

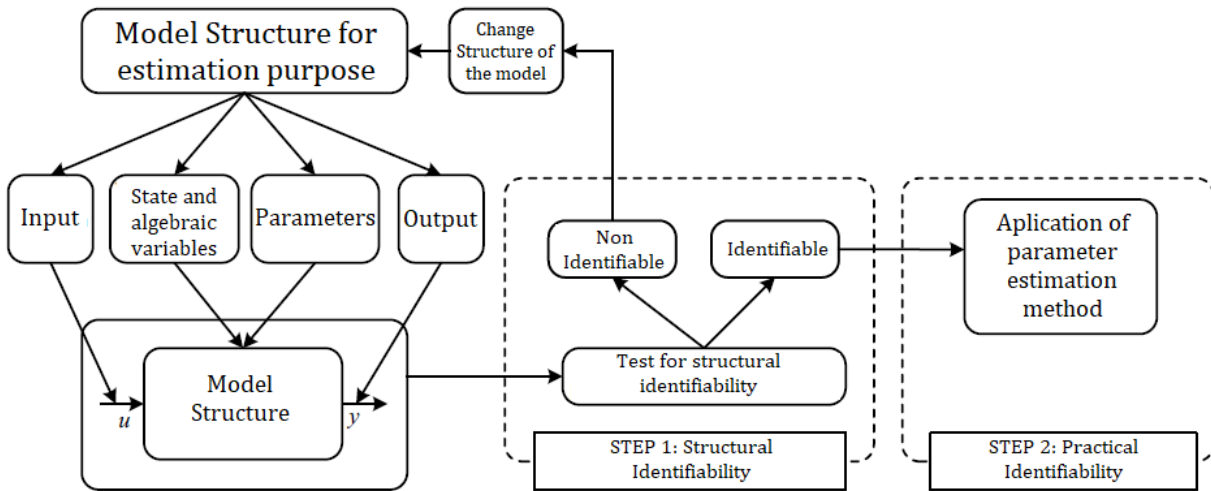


Figure 2 – Identifiability analysis proposed in (LANDGRAF, 2022)

Source: (LANDGRAF, 2022)

- Structural identifiability: In the first step of identifiability analysis, it is verified whether or not the parameter vector is identifiable from the selected inputs and outputs of the model. If the model were not identifiable, the structure of the model (inputs, state variables, parameter, output) must be altered. Such as test is fundamental especially when only the metaheuristic method is used to estimate the parameter of the model. Uniqueness problems (Non-linear methods) or convergence for unreal values for some parameters (Metaheuristic methods) can happen during the estimation process if structural identifiability is not maintained.
- Practical identifiability: After the structural identifiability is verified in Step I, the parameters of the model are obtained through a parameter estimation process. A set of parameters of the model that represents the dynamic behavior of the system with some precision have to identify, and non-linear, metaheuristic, or hybrid methods can be used in this Step.

The structural analysis of model (Eq. (2.26)-(2.29)) was successfully conducted in (LANDGRAF, 2022). Therefore, the hybrid method proposed in Section 3.2 performs

practical identifiability. More information about the identifiability analysis in a dynamic system can be found in (LANDGRAF, 2022).

3.1 Estimation process

The procedure of parameter estimation can be divided into four stages, which is proposed to make a robust and reliable estimation, where each stage has a specific function, as can be seen in Figure 4:

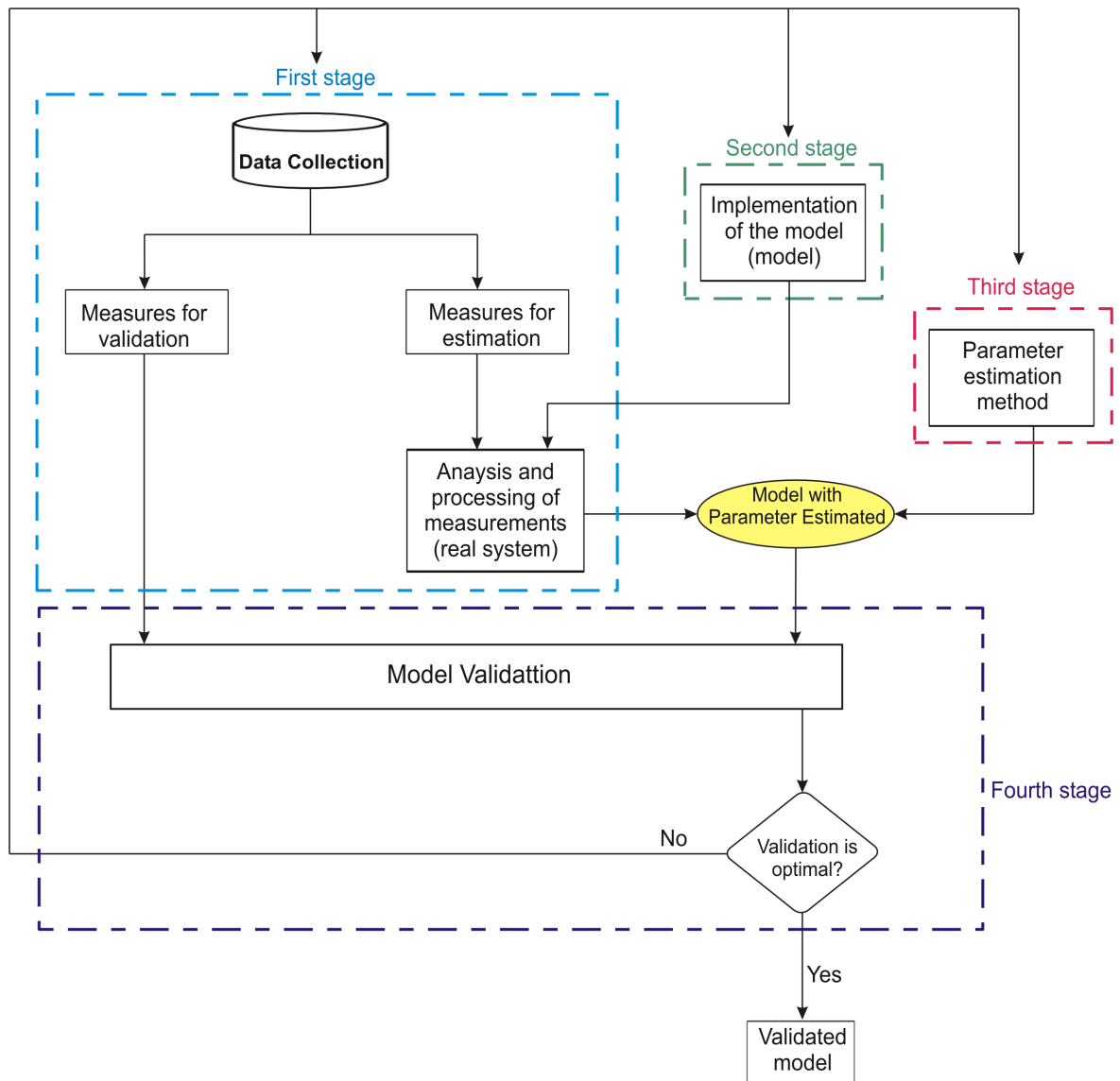


Figure 3 – Flowchart of estimation method

Source: Adapted from (CARI, 2009)

- First stage: The measurement data obtained from EES, will be gathered to get enough information about the dynamic response of the parameters.

- Second stage: The model of the system will be defined with the purpose to select the number of terms of equations, variables, etc.
- Third stage: A parameter estimation method is used to find the real value of the parameter from the available measurements of the model. In this research, a hybrid algorithm based on an evolutionary method “Mean-Variance Optimization Algorithm” (MVMO), and a non-linear programming called “Sensitivity Trajectory Method” will be used to estimate the parameters.
- Fourth stage: After the parameter estimation procedure, the validation step is performed by comparing the model outputs with those of the real system for another set of measures. In case of the validation is ok, the process stops. Otherwise, a change must be proposed to the data collection, model, or estimation method.

3.2 Hybrid Estimation Method

Let us consider the dynamic system modeled by differential-algebraic equations (DAE) given by:

$$\begin{aligned}
 \dot{x} &= f(x, z, p, u) \\
 0 &= g(x, z, p, u) \\
 y &= h(x, z, p, u)
 \end{aligned} \tag{3.1}$$

where $x \in R^m$ is the state variable vector, $y \in R^r$ is the output variable vector, $u \in R^l$ is the input variable vector, and $p \in R^{np}$ is the parameter variable vector. Let p_i be the i_{th} component of p . Functions f , g , and h must be differentiable in relation to each p_i , $i = 1, 2, \dots, np$. When the model is represented by DAEs and, according to the evolution of the parameters during the estimation, algebraic equation $g(\cdot) = 0$ of the model (3.1) can reach a bifurcation, admitting no solution and causing the method to fail. Towards solving this problem, model (3.1) is replaced by a minimization formulation in which the square of the algebraic equation is subject to differential equations (CARI; LANDGRAF; ALBERTO, 2017), (LANDGRAF, 2022).

$$\begin{aligned}
 & \min g^2(x(t), u(t), p) \\
 & \text{s.a.} \begin{cases} \dot{x}(t) = f(x(t), u(t), p) \\ x(t_0) = x_0 \end{cases} \\
 & y(t) = h(x(t), u(t), p)
 \end{aligned} \tag{3.2}$$

The values of unknown parameters are calculated through a minimization between available measurement y_r and Mathematical Model Output y (obtained from (3.2)) is formulated by a minimization problem of objective function:

$$J(p) = \frac{1}{2} \int_0^{T_0} (y_r(t) - y(t))^T (y_r(t) - y(t)) dt, \quad (3.3)$$

Where:

- $J(p)$: Objective function or fitness function
- y_r : Output vector of real system
- y : Output of the mathematical model
- T_0 : Period of the sampling of the measurement
- p : Parameter vector of the model

Towards avoiding convergence problems, (long processing time or estimation failure), the proposed method solves Eq. (3.3) in two steps, as shown in Fig. 4:

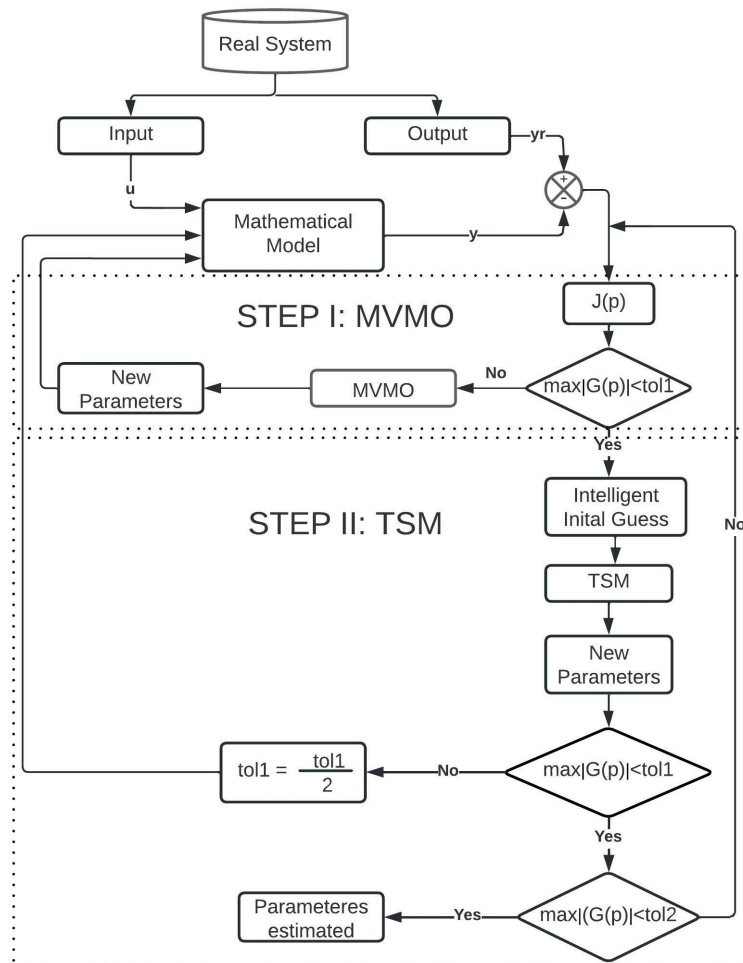


Figure 4 – Flowchart of hybrid method to parameter estimation

Source: Adapted (GOMES, 2020)

- Step I – parameter fitting by MVMO: the MVMO algorithm is used to obtain a parameter vector close to the “true value” called intelligent initial guess.
- Step II – parameter fitting by TSM: From the Intelligent initial guess provided by MVMO, the trajectory sensitivity method (TSM) is used to find the local minimum.

The steps of the hybrid parameter estimation method can be summarized as:

- Definition of the available measurements and model structure (input, output, states, parameters, and constants)
- Definition of the limits of the search region for each parameter (P_{imin}, P_{imax})
- Definition of the tolerances for MVMO (tol_1) and another for TSM (tol_2).

In Fig. 4, $G(p)$ is a vector containing the derivative of the objective function $J(p)$ related to the parameter vector, as explained in Section 3.2.2, and Tol_1 and Tol_2 are predetermined tolerances for MVMO and TSM, respectively. Since MVMO only provides an initial guess for TSM, Tol_1 is higher than Tol_2 . Towards avoiding any divergence of TSM, a maximum value of $|G(p)|$ smaller than Tol_1 should be produced. Otherwise, Tol_1 must be divided by two and MVMO must be rerun with this new tolerance.

Table 3 shows more nomenclature used in the metaheuristic method and nonlinear programming method (TSM) for a better understanding of the hybrid method. Basically, the terms "gene", "individual, and "population" used by MVMO are referred to as "parameter", "parameter vector" and "set of parameter vector", respectively.

Table 3 – Nomenclature for TSM and MVMO

| Symbol | TSM | MVMO |
|--------------------|--|---|
| $J(p)$ | Objective function | Fitness function |
| $p_i \in R$ | Parameter | gene |
| $p \in R^{np}$ | Parameter Vector $p = (p_1, p_2, \dots, p_{np})$ | Individual $Ind = (gene_1, \dots, gene_{np})$ |
| Size of population | Set of Parameter Vector | Population |
| $n_k \times n_p$ | $S_{pv} = \begin{pmatrix} Vector\ 1 \\ Vector\ 2 \\ \vdots \\ Vector\ n_k \end{pmatrix}$ | population = $\begin{pmatrix} Ind\ 1 \\ Ind\ 2 \\ \vdots \\ Ind\ n_k \end{pmatrix}$ |
| N_{ite} | Number of Iteration | Number of Generation |

The following sections detail MVMO and TSM algorithms.

3.2.1 Mean-Variance Mapping Optimization Method (MVMO)

MVMO is a metaheuristic method based on the use of a mapping function for mutating new generations with the mean and variance of the best population. The evolution of MVMO populations shares characteristics with other algorithms that also evolve. However, the method is different in the way it conducts its mutations from offspring towards diversifying the populations (ERLICH; VENAYAGAMOORTHY; WORAWAT, 2010), (GOMES; CARI, 2020), (RUEDA; ERLICH, 2018), thus updating the solution around the best one in each iteration.

First reported in (ERLICH; VENAYAGAMOORTHY; WORAWAT, 2010), it can update the parameters of the mathematical model (3.2) and reduce the fitness function (3.3).

MVMO is explained in Fig. 5 and described in the following steps:

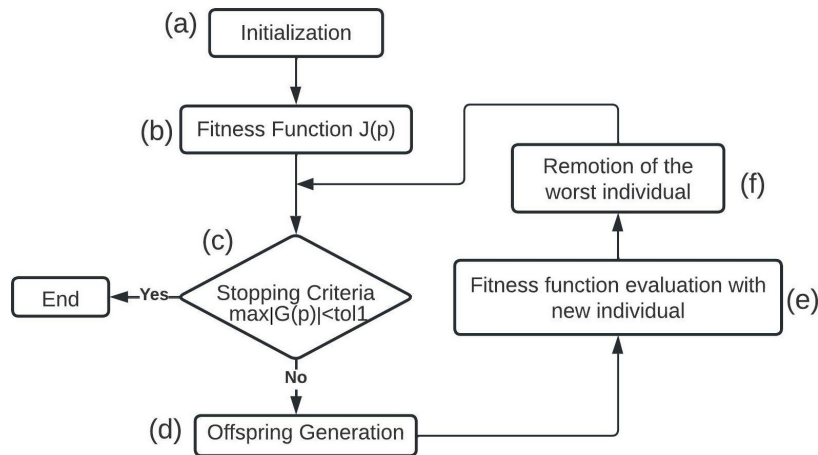


Figure 5 – Mean-variance mapping optimization

- a. Initialization: The limits of each parameter $p_i \in [p_i^{min}, p_i^{max}]$ and an individual as a parameter vector R^{np} are defined. A population is defined as a set of individuals $R^{nk} \times R^{np}$ and the number of individuals, nk , is calculated. The initial population $n_k \times n_p$ is generated tolerance, Tol_1 is defined.
- b. Fitness function evaluation: The input measures are used for computing model output y , hence, fitness function (3.3) for each individual (Ind), and ranking the population from the best (smallest $J(p)$) to the worst (largest $J(p)$). The vector is then normalized in a $[0, 1]$ range for the evolution procedure, which ensures the parameters do not lose their properties. The vectors are denormalized for each individual for the assessment of the fitness function. Mean \bar{p}_i , variance v_i , and some factors $(s_i, d_{io}, s_{i1}, s_{i2})$ (more information about MVMO algorithm process can be found in Annex B) for the population column related to each parameter are calculated

and the best individual of the population is assigned as the parent (Ind_{par}), as shown in Fig. 6.

- c. Stopping criteria: If the maximum $|G(p)|$ value of the best individual (smallest $J(p)$) is lower than Tol_1 , the method stops; otherwise, it proceeds to the next step.
- d. Offspring generation: Genes of the individual parent, Ind_{par} , are mutated by a mapping function, mean \bar{p}_i , variance v_i , and the factors ($s_i, d_{io}, d_i, s_{i1}, s_{i2}$) of the item (b) for producing a new individual (Ind_{par}). Fig. 7 illustrates the procedure.
- e. Fitness function evaluation with the new individual: The population is again ranked by a fitness function, after the inclusion of the new individual.
- f. Removal of the worst individual: the worst individual is discarded for the maintenance of the population size and returns to step "c".

| | Individuals | p_1 (gene 1) | p_2 (gene 2) | ... | p_{np} (gene np) | Fitness Function $J(p)$ | |
|-------------------------|------------------|--------------------------------|-------------------|---------------|-----------------------|----------------------------|--|
| Best ↑ ↓ Worst | Individual 1 | Individual parent: Ind_{Par} | | | | Unnormalize parameters | |
| | Individual 2 | | | | | | |
| | ⋮ | | | | | | |
| | ⋮ | Population | | | | | |
| | Individual nk | | | | | | |
| | Mean \bar{p}_i | ↓ \bar{p}_1 | ↓ \bar{p}_2 | ↓ \bar{p}_3 | ↓ \bar{p}_{np} | - | |
| | Variance v_i | ↓ v_1 | ↓ v_2 | ↓ v_3 | ↓ v_{np} | - | |
| Factors | s_i | | | | | | |
| | d_{io} | | | | | | |
| | d_i | | | | | | |
| | s_{i1} | | | | | | |
| | s_{i2} | | | | | | |

Figure 6 – Procedure, step by step, for MVMO

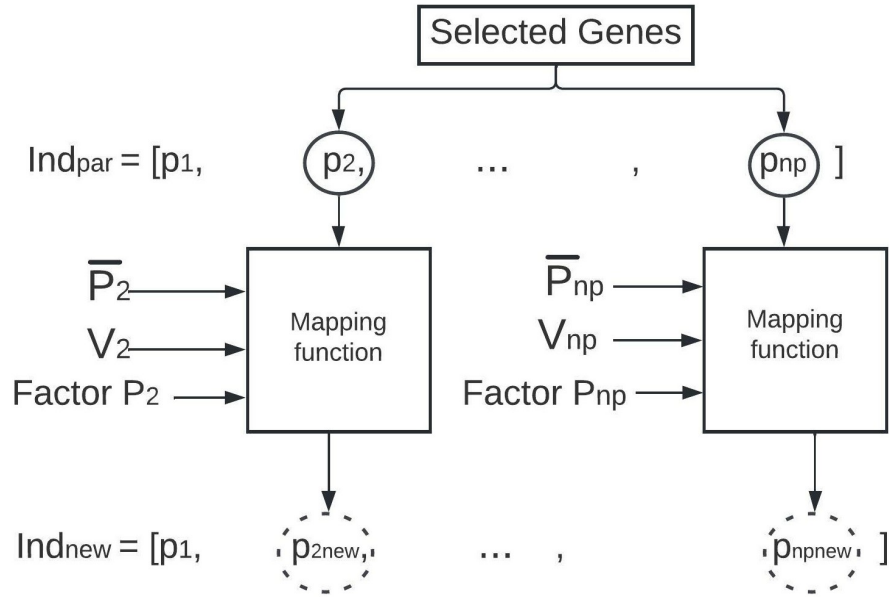


Figure 7 – New individual obtained from parent individual in offspring generator process

The main advantage of MVMO in comparison to traditional metaheuristic methods (Genetic algorithm and Particle swarm optimization) is its better performance for small populations (RUEDA; ERLICH, 2018), (GUNEN et al., 2020) -that is the reason why it is used in this research. However, like any metaheuristic method, it faces the common problem of time consumption when it is close to the local minimum. Towards overcoming it, a trajectory sensitivity method (TSM) is used in the sequence (FARIAS et al., 2018) (GOMES; CARI, 2020).

3.2.2 Trajectory Sensitivity Method

TSM is a well-established methodology for estimation purposes (BENCHLUCH; CHOW, 1993), (CARI, 2009), (CARI; LANDGRAF; ALBERTO, 2017), (FARIAS et al., 2018), and (GOMES; CARI, 2020). Compared with other nonlinear programming algorithms, in general, it has faster convergence, since it uses the Hessian of the objective function, $J(p)$, to find the solution -that is the reason why it was chosen in this research. However, like any non-linear programming method, it is highly dependent on the initial parameter guess. The problem can be solved using MVMO for obtaining a good initial guess, as explained in the previous section.

Considering the mathematical model of a dynamic system described in equation (3.2). For didactic purposes, it is rewritten here.

$$\begin{aligned}
 & \min g^2(x(t), u(t), p) \\
 & \text{s.a } \begin{cases} \dot{x}(t) = f(x(t), u(t), p) \\ x(t_0) = x_0 \end{cases} \\
 & y(t) = h(x(t), u(t), p)
 \end{aligned} \tag{3.4}$$

The estimation process can be modeled as an optimization approach so that vector p , which minimizes the objective function (3.3), can be found. Optimization condition ($\frac{\partial J(p)}{\partial p} = 0$) yields

$$G(p) = \frac{\partial J(p)}{\partial p} = - \int_0^{T_0} \left(\frac{\partial y}{\partial p} \right)^T (y_r - y) dt = 0 \quad (3.5)$$

From the initial guess and adopting the Newton-Raphson method, the parameter can be found by

$$p_{k+1} = p_k - \Gamma(p)^{-1} G(p)|_{p=p^k} \quad (3.6)$$

where Γ is the Jacobian of $G(p)$, expressed by

$$\Gamma \approx \int_0^{T_0} \left(\frac{\partial y}{\partial p} \right)^T \left(\frac{\partial y}{\partial p} \right) |_{p=p^k} \quad (3.7)$$

where $\left(\frac{\partial y}{\partial p} \right)$ is the sensitivity function which is the partial derivative of (3.2) regarding p_i . More information on TSM can be found in (BENCHLUCH; CHOW, 1993), (CARI, 2009), (FARIAS et al., 2018) and (GOMES; CARI, 2020).

4 APPLICATION AND RESULTS

In order to better understand the estimation process, first will be used the hybrid method (MVMO + TSM) on the mechanical parameters (H, D) of the synchronous generator (explained in section (2.1.4)). Next, the estimation of electrical parameters will be carried out in section 2.1.5.

The system (Fig. 8) will be evaluated with different tolerances for both the MVMO and TSM algorithms. In the case of the MVMO algorithm, the number of individuals will be analyzed. This will provide an optimal number the individuals and tolerance for use in the hybrid method.

Subsequently, the hybrid method (MVMO + TSM) will be used to estimate the electric parameters of the synchronous generator.

4.1 Mechanical Parameter Estimation

The electric energy system (EES) considered for the study is composed of a synchronous generator of 220 MVA, 24 kV, and 60 Hz that provides power to the infinite bus through a transformer and two parallel transmission lines (Fig. 8). The impedance's line, transformer, powers, and voltages values are in values per unit (p.u). The base power is 220 MVA, the based voltage on the low voltage side is 24 kV, and the high voltage side is 220 kV. The synchronous generator is composed of a cylindrical poles rotor that has an ST1A-type excitation system with $K_A = 200$, $T_A = 0.025$, $E_{fmin} = -6.4$, and $E_{fmax} = 7$. The experimental data were obtained from a short circuit in one of the terminals of the L_2 . The disturbance is eliminated by the protection devices in the time $t=0.07$ s.

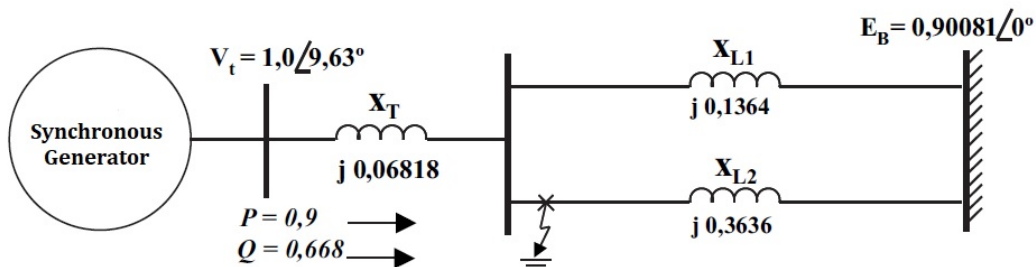


Figure 8 – Electric power system for testing the mechanical parameters

Source: (LANDGRAF, 2014)

4.1.1 Benchmark for mechanical parameter estimation

In order to compare the result of the estimative provided by the hybrid method, the mechanical generator parameter obtained in (LANDGRAF, 2014) was used as a benchmark (see Table 4).

Table 4 – Mechanical Parameters of Generator of 220 MVA obtained of (LANDGRAF, 2014) used as benchmark

| Parameter | H | D |
|-----------|-----|--------|
| Value | 3.5 | 0.0024 |

For comparison purposes, initially, the mechanical generator parameters were estimated by MVMO and TSM independently. The proposed hybrid method was then used for the same purpose.

4.1.2 Estimation of mechanical parameters with MVMO

MVMO estimated the mechanical parameters of the synchronous generator of 220 MVA using the following features

| | |
|---|---------------------------------------|
| Number of gens, n_p : | 2 |
| Number of gens for mutation, n_{gm} : | 2 |
| Number of individuals, n_k : | 10 (for case 1) and 50 (for case 2) |
| Tolerance, Tol_1 : | 0.5; 0.1; 0.01 (for three situations) |

Two cases were analyzed using two different numbers of individuals 10 (Case 1) and 50 (Case 2) to find the optimal number of individuals. In addition, three different tolerances (0.5, 0.1, and 0.01) were used for each case. The summary of the results using 10 and 50 individuals can be seen in Table 5 and 6, respectively.

Table 5 – Results of MVMO for 10 individuals (Case 1)

| Tol_1 | Par. | Final Value | Reference Values (LANDGRAF, 2014) | Error % | Time |
|---------|-------------------|-------------|--------------------------------------|---------|-------|
| 0.5 | $0 \leq H \leq 7$ | 4.07 | 3.5 | 48.4 | 27 s |
| | $0 \leq D \leq 1$ | 0.026 | 0.0024 | 57.1 | |
| 0.1 | $0 \leq H \leq 7$ | 3.38 | 3.5 | 23.4 | 43 s |
| | $0 \leq D \leq 1$ | 0.0047 | 0.0024 | 37.4 | |
| 0.01 | $0 \leq H \leq 7$ | 3.48 | 3.5 | 6.75 | 1 min |
| | $0 \leq D \leq 1$ | 0.0026 | 0.0024 | 8.4 | |

Table 6 – Results of MVMO for 50 individuals (Case 2)

| Tol_1 | Par. | Final Value | Reference Values (LANDGRAF, 2014) | Error % | Time |
|---------|-------------------|-------------|--------------------------------------|---------|-------|
| 0.5 | $0 \leq H \leq 7$ | 3.15 | 3.5 | 13.4 | 46 s |
| | $0 \leq D \leq 1$ | 0.013 | 0.0024 | 48.7 | |
| 0.1 | $0 \leq H \leq 7$ | 3.347 | 3.5 | 4.12 | 1 min |
| | $0 \leq D \leq 1$ | 0.0075 | 0.0024 | 36.2 | 8 s |
| 0.01 | $0 \leq H \leq 7$ | 3.49 | 3.5 | 0.22 | 2 min |
| | $\leq D \leq 1$ | 0.0027 | 0.0024 | 3.45 | 5 s |

Based on the result of Table 5 and 6, it was concluded that the error between the reference and estimated parameter values becomes smaller as the tolerance decreases when using 10 and 50 individuals for MVMO. However, the processing time also increases. Additionally, when is used 50 individuals (Table 6) the accuracy of the estimated parameter was improved. Nonetheless, the processing time also increased.

4.1.3 Estimation of mechanical parameters with TSM

TSM estimated the mechanical parameters of the 220 MVA synchronous generator. The initial guess, for the two cases, was obtained from a difference of ± 10 and ± 30 of the reference parameter (Table 4), and the tolerance for both cases was $Tol_2 = 0.001$. Tables 7 and 8 show the results for both cases.

Table 7 – Results of TSM from initial guess with a difference ± 10 of the reference parameter

| Par. | Initial Guess | Final Values | Ref. Values (LANDGRAF, 2014) | Error % Values | Time (s) |
|------|---------------|--------------|---------------------------------|-------------------|-------------|
| H | 5.25 | 3.5 | 3.5 | 0 | 3.2 s |
| D | 0.0048 | 0.0024 | 0.0024 | 0 | |

Table 8 – Results of TSM from initial guess with a difference ± 30 of the reference parameter

| Par. | Initial Guess | Final Values | Ref. Values (LANDGRAF, 2014) | Error % Values | Time (s) |
|------|---------------|--------------|---------------------------------|-------------------|-------------|
| H | 7 | 3.5 | diverge | - | - |
| D | 0.006 | 0.0024 | diverge | - | |

As can be seen in Table 7, the accuracy of the parameter estimated by TSM is better than the MVMO method. In addition, the time processing is also smaller. However, the TSM has a strong dependency on the initial guess value, as can be seen in Table 8.

4.1.4 Results of Hybrid Method

The hybrid method estimated the mechanical parameters of the synchronous generator. MVMO just provided an intelligent guess for TSM, as addressed in Section 3.2, using the following features:

| | |
|---|-------|
| Number of gens, n_p : | 2 |
| Number of gens for mutation, n_{gm} : | 2 |
| Number of individuals, n_k : | 10 |
| Tolerance MVMO, Tol_1 : | 0.5 |
| Tolerance TSM, Tol_2 : | 0.001 |

Table 9 shows the results of the application of the hybrid method for estimating the mechanical parameters. The final value obtained by MVMO with a tolerance Tol_1 was used as an intelligent initial guess for TSM (gray column). The method converges in 36 s.

Since the final value of MVMO depends on the first population randomly generated from the search region, the hybrid method was executed ten times. In all cases, the parameter converged to the reference value and the processing time ranged between 35 and 40 seconds.

Table 9 – Hybrid method results

| | Par. | Intelligent Ini. guess | Tol 1 | Final Value | Ref. Value | Error % | Time (s) |
|----------------|------|------------------------|-------|-------------|------------|---------|----------|
| MVMO | H | $0 \leq H \leq 7$ | 0.5 | 3.77 | 3.5 | 34.4 | 29 |
| | D | $0 \leq D \leq 1$ | | 0.005 | | | |
| | Par. | Intelligent Ini. guess | Tol 2 | Final Value | Ref. Value | Error % | Time (s) |
| TSM | H | 3.77 | 0.001 | 3.5 | 3.5 | 0 | 7 |
| | D | 0.005 | | 0.0024 | 0.0024 | 0 | |
| Total Time (s) | | | | | | | 36 |

The hybrid method makes the estimation process reliable and robust regarding convergence problems.

Figure 9 displays a comparison between the outputs signal (w) of the initial model (before the estimation process) with the dashed line with the final model (after the estimation process) with a red line for real measures and blue points line for the mathematical model, respectively. After the application of the hybrid method, the output of the real and mathematical model system was close enough, implying a correct estimation.

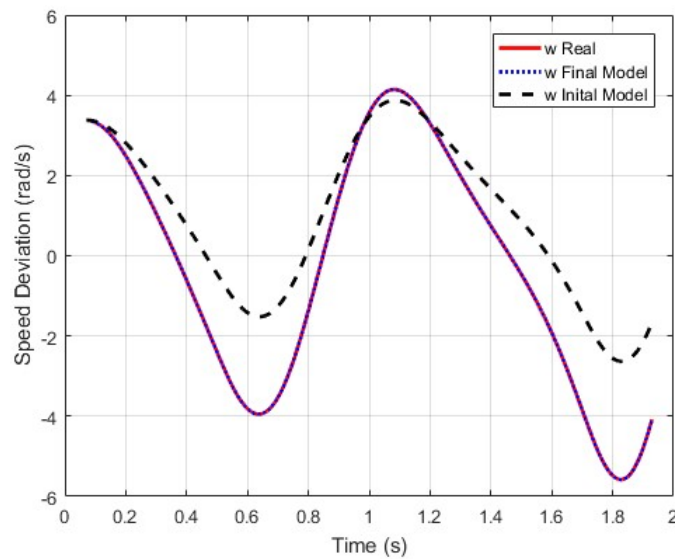


Figure 9 – Initial and final estimation process of the mechanical parameters with the hybrid method

4.2 Electric Parameter Estimation

The results obtained in this section were obtained through two EES built in a laboratory. The measurements for the estimation will be obtained from a small power system to apply the hybrid method in a computer with a capacity of 32 Gb of RAM.

The electric system test was built for obtaining experimental measurement data with a synchronous generator connected to two loads through a transmission line (see Fig. 10). The dynamic load is composed of a capacitor bank and a three-phase induction motor and the synchronous generator (SG) have 4 poles, 2 KVA, 220 V, 60 Hz, and Y connected. The experimental data were obtained from a) a sudden connection of a dynamic load and b) a sudden load disconnection (Table 10).

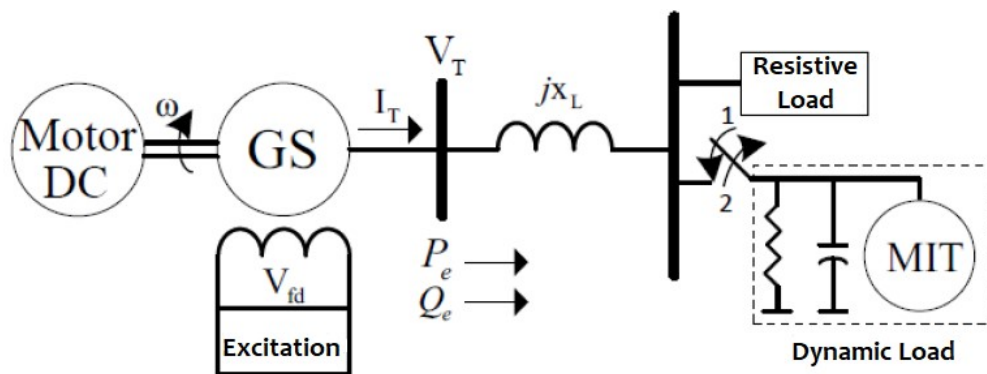


Figure 10 – Electric Power System built for the obtaining of measurement data for electric parameters

Source: (LANDGRAF, 2022)

Table 10 – Information on disturbances data obtained from (CARI; LANDGRAF; ALBERTO, 2017)

| Disturbances | Use | $t_{ini}(s)$ | $t_f(s)$ |
|-----------------------------|------------|--------------|----------|
| 1.Sudden load connection | Estimation | 0.46 | 2.98 |
| 2.Sudden load disconnection | Validation | 0.26 | 2.48 |

The bases for the obtaining of per unit values (p.u) were nominal value of power (2 KVA) and line voltage (220 V).

4.2.1 Benchmark for parameter and optimal time period

The generator parameter obtained in (LANDGRAF, 2022) was used as a benchmark (see Table 11) for comparisons of the estimation results provided by the hybrid method.

Table 11 – Parameter of 2KVA Generator obtained from (LANDGRAF, 2022) and used as a benchmark

| Parameter | x_d | x'_d | T'_{d0} | x_q | K_e | E'_{q0} |
|-----------|-------|--------|-----------|-------|-------|-----------|
| Value | 1.14 | 0.45 | 0.22 | 0.57 | 84.22 | 1.03 |

The optimal time windows for the measurement data were $t_{ini} = 0.46s$ (initial time of the disturbance) and $t_{fin} = 2.06s$, according to the procedure proposed in (LANDGRAF; CARI; ALBERTO, 2022).

4.2.2 Parameter Limits for the generator

MVMO depends on a careful selection of the search region in the parameter space to succeed in the estimation. Therefore, the parameter limits provided by (KUNDUR, 1994) (see Table 12, Column 2) can be used by generators with more than 10 MVA. However, they may not be adequate for smaller synchronous generators with less than 10 MVA, especially for T'_{d0} , since small ones have small inertia, which influences such parameters. Towards general parameter limits, the values provided by (KUNDUR, 1994) were expanded, as shown in column 3 of Table 12.

Table 12 – Parameter limits in p.u. for salient pole rotor used for MVMO

| Parameter | Provided by (KUNDUR, 1994) | Used in this study |
|-----------|----------------------------|--------------------|
| x_d | 0.6 - 1.5 | 0.6 - 1.5 |
| x'_d | 0.2 - 0.5 | 0.2 - 0.5 |
| T'_{d0} | 1.5 - 9.0 | 0.1 - 9.0 |
| x_q | 0.4 - 1.0 | 0.4 - 1.0 |
| K_e | — | 50 - 90 |
| E'_{q0} | — | 0.7 - 1.3 |

The limits for K_e and E'_{q0} were obtained by the deviation of the nominal values of the field voltage and terminal voltage (in p.u.), respectively. When the individuals

(parameter vector) are randomly obtained (Table 12) for MVMO, the physical constraint of the synchronous generator must be obeyed: $x_d > x_q > x'_d$.

4.2.3 Procedure for electric Parameter Estimation

For comparison purposes, initially, the generator parameters were estimated by MVMO and TSM independently. The proposed hybrid algorithm was then used for the same purpose.

4.2.3.1 Parameter Estimation by MVMO

MVMO estimated the parameter of the 2 KVA synchronous generator using the following features:

| | |
|---|---------------------------------------|
| Number of gens, n_p : | 6 |
| Number of gens for mutation, n_{gm} : | 2 |
| Number of individuals, n_k : | 10 (for case 1) and 50 (for case 2) |
| Tolerance, Tol_1 : | 0.5; 0.1; 0.01 (for three situations) |

Two cases were analyzed with two different numbers of individuals, i.e., 10 (Case 1) and 50 (Case 2) so that the optimal number of individuals could be found. Three different tolerances (0.5, 0.1, and 0.01) were used for each case. Tables 13 and 14 show a summary of the results from the use of 10 and 50 individuals, respectively.

Table 13 – Results of MVMO for 10 individuals (Case 1)

| Tol ₁ | Par. | Final Value | Reference Values (LANDGRAF, 2014) | Error % | Time |
|------------------|-----------|-------------|-----------------------------------|---------|---------------|
| 0.5 | x_d | 1.10 | 1.14 | 0.87 | 53.27 s |
| | x'_d | 0.44 | 0.45 | 2.2 | |
| | T'_{d0} | 0.20 | 0.22 | 4.54 | |
| | x_q | 0.56 | 0.57 | 1.75 | |
| | K_e | 83.9 | 84.22 | 0.2 | |
| | E'_q | 1.05 | 1.03 | 0.97 | |
| 0.1 | x_d | 1.15 | 1.14 | 0.52 | 2 min 34 s |
| | x'_d | 0.44 | 0.45 | 2.2 | |
| | T'_{d0} | 0.222 | 0.22 | 0.9 | |
| | x_q | 0.576 | 0.57 | 1.22 | |
| | K_e | 83.92 | 84.22 | 0.28 | |
| | E'_q | 1.04 | 1.03 | 0.96 | |
| 0.01 | x_d | 1.141 | 1.14 | 0.08 | 6 min 13 s |
| | x'_d | 0.445 | 0.45 | 0.01 | |
| | T'_{d0} | 0.221 | 0.22 | 0.45 | |
| | x_q | 0.572 | 0.57 | 0.35 | |
| | K_e | 84.12 | 84.22 | 0.11 | |
| | E'_q | 1.04 | 1.03 | 0.97 | |

As expected, the error between the reference and estimated parameter values becomes smaller as the tolerance decreases when 10 individuals are used (Table 5). However, the processing time also increases.

Similarly, when MVMO used 50 individuals (Table 14), the accuracy of the estimated parameter was improved. Nonetheless, the processing time was also increased.

Table 14 – Results of MVMO for 50 individuals (Case 2)

| Tol ₁ | Par. | Final Value | Reference Values (LANDGRAF, 2014) | Error % | Time |
|------------------|-----------|-------------|-----------------------------------|---------|-----------------|
| 0.5 | x_d | 1.148 | 1.14 | 0.7 | 2 min 41 s |
| | x'_d | 0.48 | 0.45 | 6.6 | |
| | T'_{d0} | 0.225 | 0.22 | 2.27 | |
| | x_q | 0.578 | 0.57 | 1.40 | |
| | K_e | 84.15 | 84.22 | 0.19 | |
| | E'_q | 1.032 | 1.03 | 0.19 | |
| 0.1 | x_d | 1.147 | 1.14 | 0.61 | 7 min s 30 s |
| | x'_d | 0.451 | 0.45 | 0.22 | |
| | T'_{d0} | 0.228 | 0.22 | 3.63 | |
| | x_q | 0.5776 | 0.57 | 1.22 | |
| | K_e | 84.09 | 84.22 | 0.15 | |
| | E'_q | 1.04 | 1.03 | 0.97 | |
| 0.01 | x_d | 1.141 | 1.14 | 0.08 | 12 min 24 s |
| | x'_d | 0.449 | 0.45 | 0.22 | |
| | T'_{d0} | 0.228 | 0.22 | 3.63 | |
| | x_q | 0.577 | 0.57 | 1.22 | |
| | K_e | 84.27 | 84.22 | 0.05 | |
| | E'_q | 1.035 | 1.03 | 0.004 | |

According to Tables 13 and 14, ten individuals and 0.5 tolerance are enough for MVMO to obtain a good initial estimate of the parameters.

4.2.3.2 Results of TSM

TSM estimated the parameter of the 2 kVA synchronous generator. The initial guess, for the two cases, was obtained from a difference of ± 10 and ± 30 of the reference parameter (Table 11). The initial guess for E_{q0} was V_{T0} (Terminal voltage in p.u.), as recommended by (LANDGRAF; CARI; ALBERTO, 2022). Physical constraint $x'_d < x_q < x_d$ was obeyed and the tolerance for both cases was $tol_2 = 0.001$. Tables 15 and 16 show the results of the two cases.

The accuracy of the parameter estimated by TSM is better than that obtained by MVMO and the time processing is shorter. However, TSM is highly dependent on the initial guess value. The parameter diverges for an initial guess distant from the reference value (see in Table 16).

Table 15 – Results of TSM from initial guess with a difference ± 10 of the reference parameter value

| Par. | Initial Guess | Final Values | Reference Values (LANDGRAF, 2014) | Error % (s) | Time |
|-----------|---------------|--------------|--------------------------------------|----------------|-------|
| x_d | 1.25 | 1.142 | 1.14 | 0 | 13.02 |
| x'_d | 0.49 | 0.45 | 0.45 | 0 | |
| T'_{d0} | 0.24 | 0.22 | 0.22 | 0 | |
| x_q | 0.62 | 0.57 | 0.57 | 0 | |
| K_e | 92.28 | 84.2 | 84.22 | 0 | |
| E'_q | $V_{T0}=1.12$ | 1.032 | 1.03 | 0 | |

Table 16 – Results of TSM from initial guess with a difference ± 30 of the reference parameter value

| Par. | Initial Guess | Final Values | Reference Values (LANDGRAF, 2014) | Error % (s) | Time |
|-----------|---------------|--------------|--------------------------------------|----------------|------|
| x_d | 1.36 | Diverge | 1.14 | - | - |
| x'_d | 0.55 | Diverge | 0.45 | - | |
| T'_{d0} | 0.25 | Diverge | 0.22 | - | |
| x_q | 0.67 | Diverge | 0.57 | - | |
| K_e | 101.26 | Diverge | 84.22 | - | |
| E'_q | $V_{T0}=1.12$ | Diverge | 1.03 | - | |

Different initial values were randomly obtained from Table 12 for the evaluation of the influence of initial guess on TSM convergence. Physical constraint $x'_d < x_q < x_d$ was kept. Table 17 shows the results for ten cases.

Table 17 – Convergence of TSM for different initial guesses from limits of Table 12

| Initial guess | x_d | x'_d | T'_{d0} | x_q | K_e | E'_q | Converge |
|---------------|-------|--------|-----------|-------|-------|--------|----------|
| Set 1 | 1.21 | 0.49 | 0.24 | 0.58 | 83 | 0.98 | Yes |
| Set 2 | 0.9 | 0.42 | 0.45 | 0.6 | 89 | 1 | Yes |
| Set 3 | 1.4 | 0.37 | 2.8 | 0.9 | 75 | 1.1 | No |
| Set 4 | 0.75 | 0.33 | 3.9 | 0.64 | 66 | 0.85 | No |
| Set 5 | 0.62 | 0.44 | 4.5 | 0.5 | 85 | 0.94 | No |
| Set 6 | 1.3 | 0.3 | 1.5 | 0.75 | 70 | 0.9 | Yes |
| Set 7 | 0.85 | 0.21 | 0.55 | 0.75 | 52 | 0.75 | No |
| Set 8 | 1 | 0.49 | 1.03 | 0.92 | 60 | 1.2 | No |
| Set 9 | 1.3 | 0.27 | 3 | 0.7 | 58 | 0.8 | No |
| Set 10 | 0.8 | 0.4 | 0.9 | 0.8 | 64 | 1.25 | No |

4.2.3.3 Results of Hybrid Method

The hybrid method estimated the generator parameter. MVMO only provided an intelligent initial guess for TSM, as addressed in chapter 2.1, using the following features:

| | |
|---|-------|
| Number of gens, n_p : | 6 |
| Number of gens for mutation, n_{gm} : | 2 |
| Number of individuals, n_k : | 10 |
| Tolerance MVMO, Tol_1 : | 0.5 |
| Tolerance TSM, Tol_2 : | 0.001 |

Table 18 shows the result of the application of the hybrid method for estimating the parameter.

The final value obtained by MVMO for tolerance (Tol_1) 0.5 was used as an intelligent initial guess for TSM (gray columns). The parameters converged to the reference values in 63.73 seconds.

Since the final value of MVMO depends on the first population randomly generated from the search region, the hybrid method was applied twenty times. In all cases, the parameter converged to the reference value and the processing time ranged between 55 and 75 seconds.

Table 18 – Hybrid method results

| | Par. | Search region | Tol 1 | Final Value | Ref. Value | Error % | Time (s) |
|----------------|-----------|---------------------------|-------|-------------|------------|---------|----------|
| MVMO | x_d | $0.6 \leq x_d \leq 1.5$ | 0.5 | 1.13 | 1.14 | 0.78 | 50.48 |
| | x'_d | $0.2 \leq x'_d \leq 0.5$ | | 0.46 | 0.45 | 1.45 | |
| | T'_{d0} | $0.1 \leq T'_{d0} \leq 9$ | | 0.23 | 0.22 | 3.56 | |
| | x_q | $0.4 \leq x_q \leq 1$ | | 0.59 | 0.57 | 2.34 | |
| | K_e | $50 \leq K_e \leq 90$ | | 83.4 | 84.22 | 0.64 | |
| | E'_q | $0.7 \leq E'_q \leq 1.3$ | | 1.1 | 1.03 | 6.36 | |
| | Par. | Intelligent Ini. guess | Tol 2 | Final Value | Ref. Value | Error % | Time (s) |
| TSM | x_d | 1.13 | 0.001 | 1.14 | 1.14 | 0 | 13.25 |
| | x'_d | 0.46 | | 0.45 | 0.45 | 0 | |
| | T'_{d0} | 0.23 | | 0.22 | 0.22 | 0 | |
| | x_q | 0.59 | | 0.57 | 0.57 | 0 | |
| | K_e | 83.4 | | 84.2 | 84.2 | 0 | |
| | E'_q | 1.1 | | 1.03 | 1.03 | 0 | |
| Total Time (s) | | | | | | | 63.73 |

The hybrid method makes the estimation process reliable and robust regarding convergence problems.

Fig. 11a and 11b display a comparison between the output signals (P_e and Q_e) of the real system (continuous line) with the mathematical model (dashed line), respectively. After the application of the hybrid method, the outputs of both actual and model systems were close enough, implying a correct estimation.

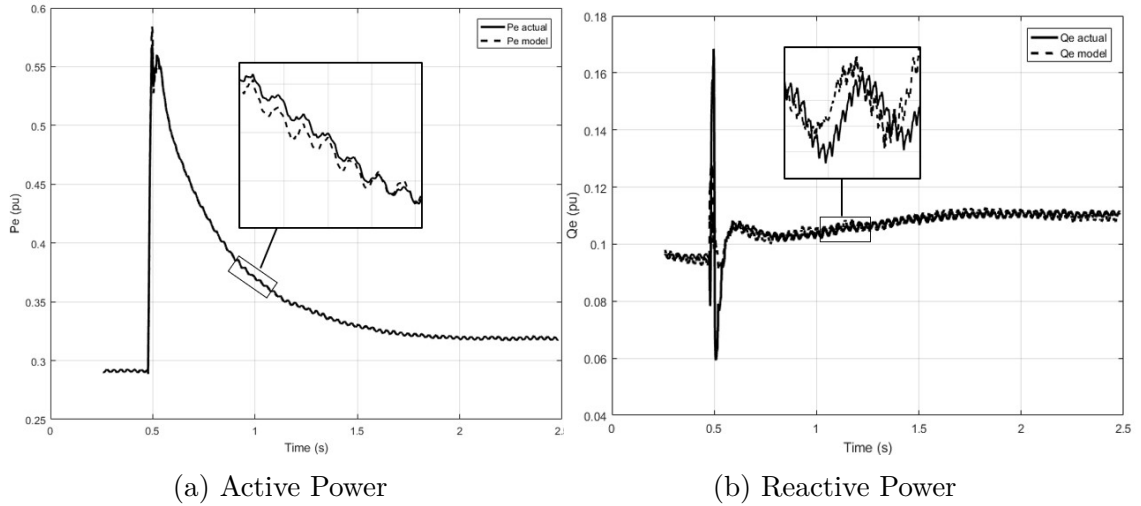


Figure 11 – Outputs of EES after the parameter fitting of the Hybrid Method

4.2.3.4 Validation results

The output of the model (Eq. 2.26 - 2.29) was simulated with the use of the estimated parameter of Table 18 with input vector $u = [I_t, V_T, Q_e]$ of the second type of disturbance data explained in section 4.2. Figs. 12a and 12b show the output of the real system (actual) and the mathematical model (model) of the validation. Both output model and actual system are close enough, as expected by a correct estimation.

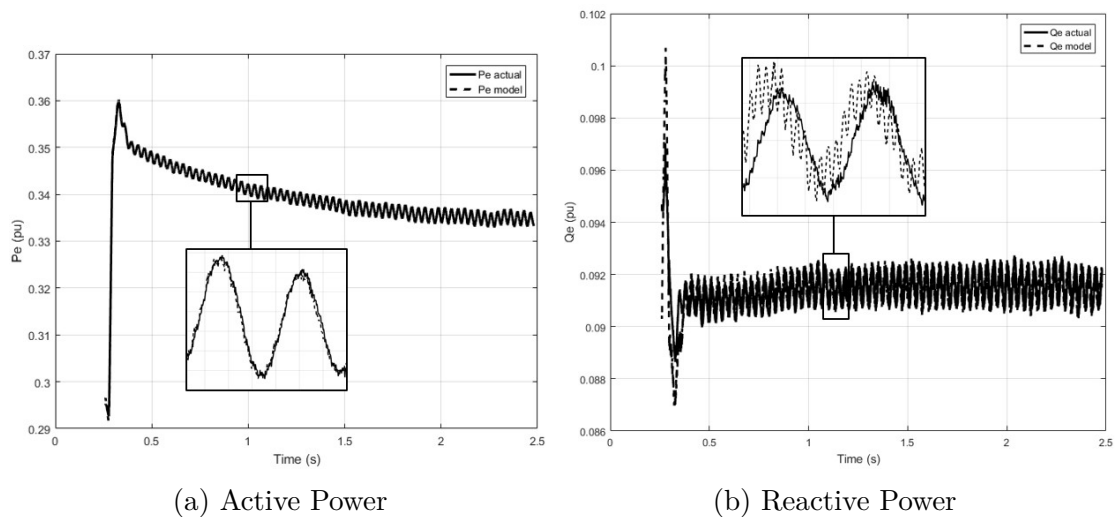


Figure 12 – Outputs of EES for validation results provided by the Hybrid Method

5 SOFTWARE FOR PARAMETER ESTIMATION OF SYNCHRONOUS GENERATOR - GENVALIDA 1.0.

In order to estimate, the parameters of the one-axis transient generator model of chapter 2, a software with a Graphical User Interface (GUI) was developed in C-Sharp (C#), the software called "Genvalida 1.0." provides a toolbox and customize framework for parameter estimation with the built-in mathematical model an estimation MVMO and TSM methods.

The GUI of the software was developed in three parts:

- Initial screen.
- Mechanical Parameter Screen: Contains the estimation of mechanical parameters of synchronous generator model of section 2.1.4.
- Electric Parameter Screen: Contains the estimation of electric parameters of the one-axis transient model of synchronous generator model of section 2.1.5.

5.1 Initial screen

The initial screen for the GUI for parameter estimation presents the following parts:

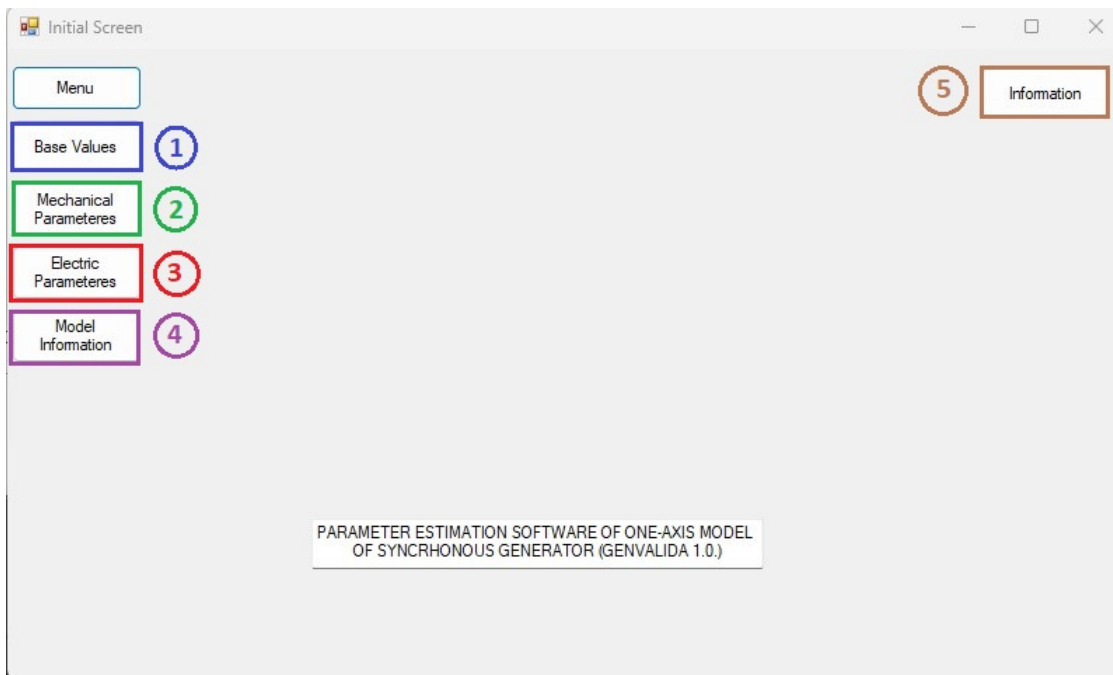


Figure 13 – Mechanical Parameter Estimation GUI

- a. The first tool (1) is used to select the base values in p.u., which the electric power system is working.
- b. The mechanical parameter GUI can be opened through the button (2).
- c. The third button (3) will be used to open the electric parameters GUI.
- d. The information about the model of the synchronous generator for estimation purposes can be obtained through the button (4).
- e. The fifth button (5) shows information about how the hybrid method works.

5.2 Mechanical Parameters GUI

A GUI was developed for mechanical parameters, such as presented in subsection 2.1.4, as can be seen in Fig. 14:

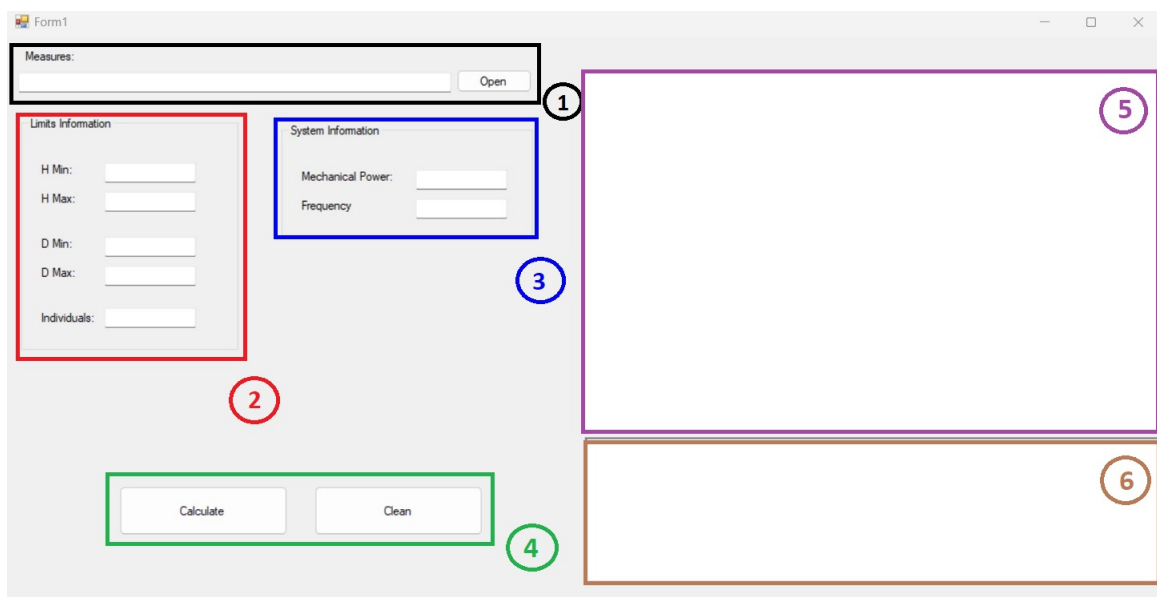


Figure 14 – Mechanical Parameter Estimation GUI

Fig. 14 shows how is distributed the GUI for mechanical parameters, where:

- a. The first number is used to select the file containing the measured data used in the estimation process.
- b. The second number is where the limits are defined for the parameter search region to find the intelligent initial guess
- c. The third number contains the system information.
- d. The fourth number contains the buttons to make the hybrid parameter estimation.

- e. The fifth number shows the graphics between the mathematical model and the real measures.
- f. The sixth number shows the results of the hybrid estimation method, where the final parameters can be found.

The GUI with results of the mechanical parameter estimation can be found in Fig.

15:

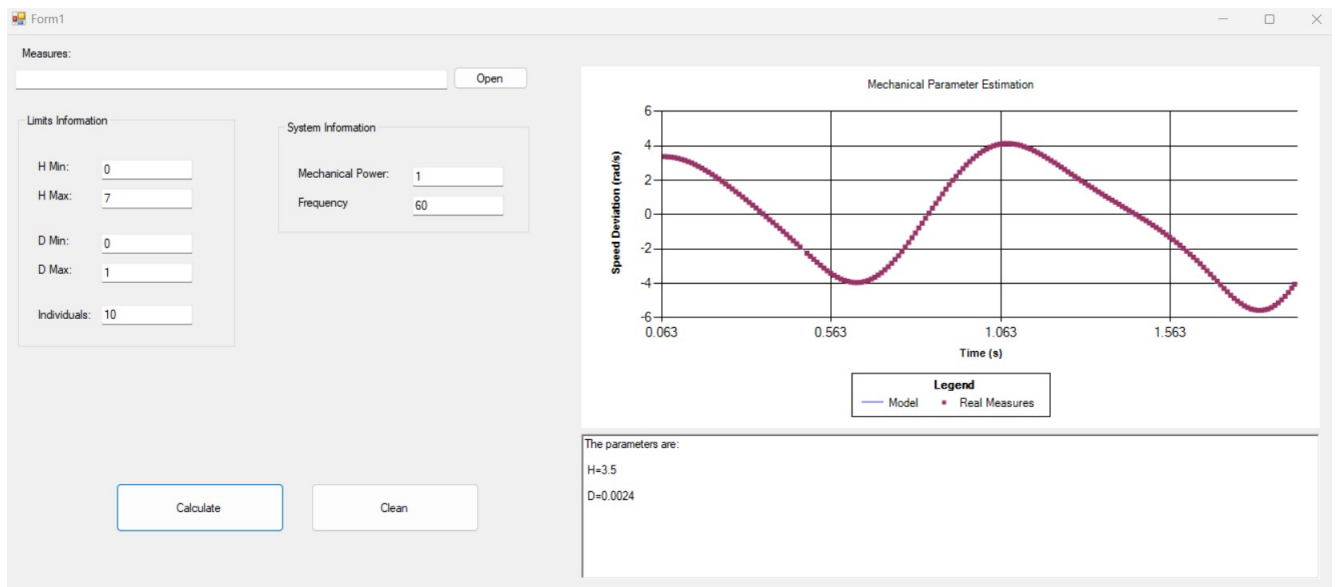


Figure 15 – Results of the Mechanical Parameter Estimation GUI

5.3 Electric Parameters GUI

The second part of the GUI is the electric parameter estimation explained in subsection 2.1.5, as can be seen in Fig. 16.

In the same way that mechanical parameters GUI, the electric parameters are divided into sections:

- a. The first section is used to select the file containing the measured data used in the estimation process.
- b. The second section is where the limits are defined for the parameter search region to find the intelligent initial guess
- c. The third section contains the buttons to make the hybrid parameter estimation.
- d. The fourth section shows the graphics between the mathematical model and the real measures.

- e. The fifth section shows the results of the hybrid estimation method, where the final parameters can be found.

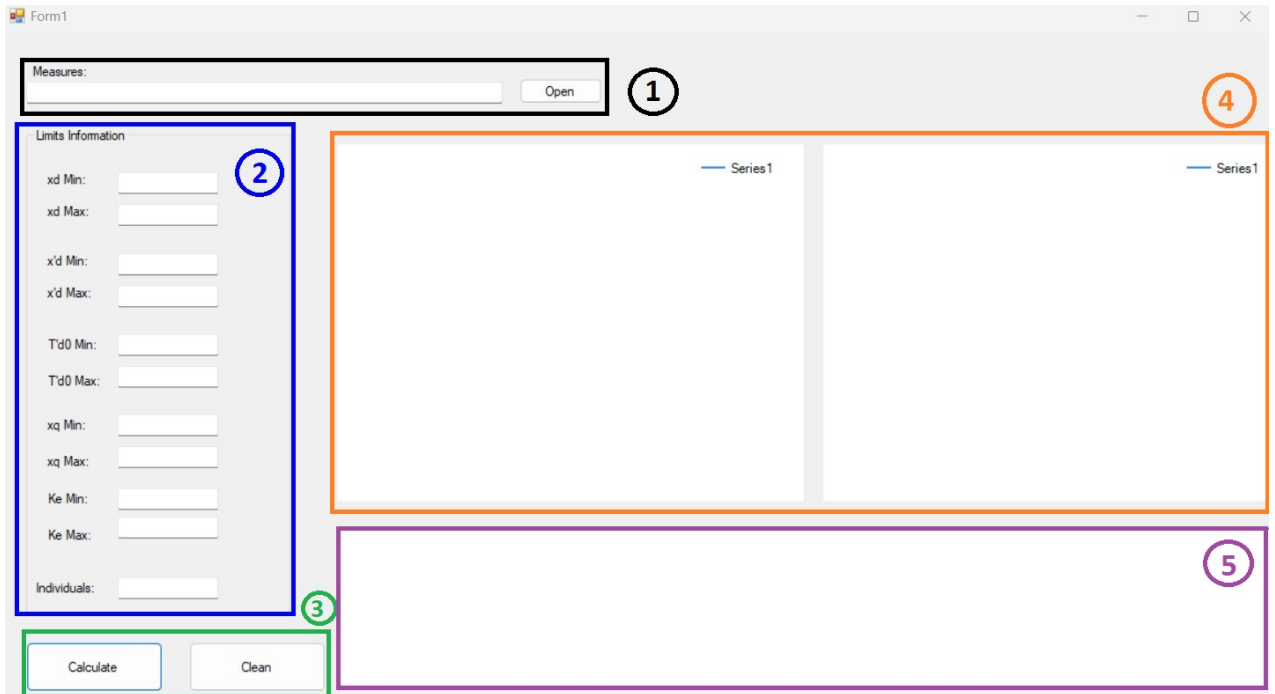


Figure 16 – Results of the Mechanical Parameter Estimation GUI

The results of the electric parameter estimation in the GUI can be found in Fig. 17:

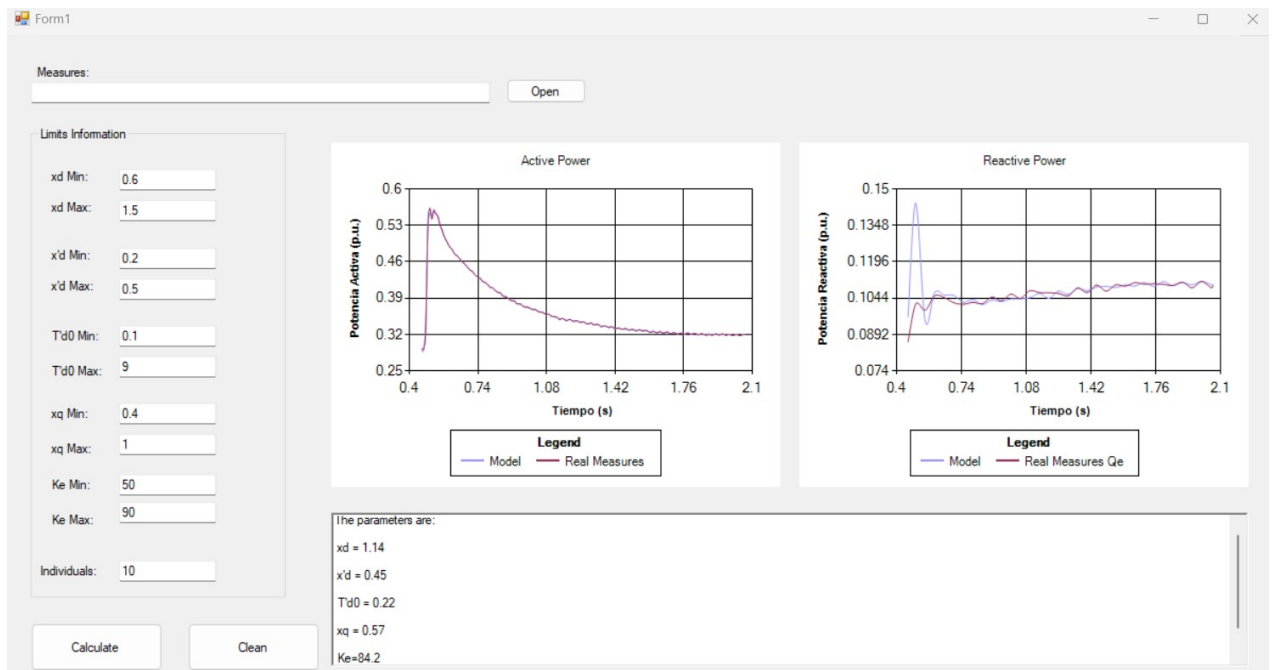


Figure 17 – Results of the electrical Parameter Estimation GUI

6 CONCLUSIONS

A hybrid method based on "Mean-Variance Optimization Method (MVMO)" (metaheuristic algorithm) and "Trajectory Sensitivity Method (TSM)" (nonlinear programming method) has been proposed for the parameter estimation of the one-axis transient generator model.

The method is applied in two steps. Initially, the metaheuristic algorithm is executed for providing an intelligent initial guess for the second algorithm. A nonlinear programming method is then applied using the initial guess so that the local minimum can be found.

The method was applied to the mechanical and electric parameters of the synchronous generator with successful results.

The method was tested regarding processing time, accuracy, and convergence of the parameters. The results show the accuracy of the estimated parameter and guarantee convergence, providing a robust and reliable estimation process.

In addition, a software with a friendly interface (GUI) was developed with the hybrid method.

6.1 Ongoing research

Ongoing research has been conducted towards the application of the hybrid method (MVMO + TSM) to other generator models such as the two-axis model and sub-transient model.

6.2 Published works

- Vigoria M. E. F; Cari, E. P. T. - Hybrid Estimation of Mechanical Parameters of Synchronous Generator (Accepted XIX ERIAC)
- Vigoria M. E. F; Cari, E. P. T. - A hybrid method for the parameter estimation of one-axis generators model (Submitted)

BIBLIOGRAPHY

ADKINS, B.; HARLEY, R. G. **The general theory of alternating current machines: application to practical problems**. [S.l.]: Springer, 2013.

ANDERSON, P. M.; FOUAD, A. A. **Power system control and stability**. [S.l.]: John Wiley & Sons, 2008.

BEHNAM-GUILANI, K. Digital modeling of synchronous machines for transient stability studies[ph. d. thesis]. 1980.

BENCHLUCH, S. M.; CHOW, J. H. A trajectory sensitivity method for the identification of nonlinear excitation system models. **IEEE Transactions on Energy Conversion**, IEEE, v. 8, n. 2, p. 159–164, 1993.

BLUM, C.; ROLI, A. Metaheuristics in combinatorial optimization: Overview and conceptual comparison. **ACM computing surveys (CSUR)**, Acm New York, NY, USA, v. 35, n. 3, p. 268–308, 2003.

BURTH, M.; VERGHESE, G. C.; VELEZ-REYES, M. Subset selection for improved parameter estimation in online identification of a synchronous generator. **IEEE Transactions on Power Systems**, IEEE, v. 14, n. 1, p. 218–225, 1999.

CARI, E. P.; LANDGRAF, T. G.; ALBERTO, L. F. A constrained minimization approach for the estimation of parameters of transient generator models. **Electric Power Systems Research**, Elsevier, v. 143, p. 252–261, 2017.

CARI, E. P. T. **Estimação dos parâmetros da máquina síncrona e seu sistema de excitação**. 2005. Dissertação (Mestrado) — Universidade de São Paulo, 2005.

CARI, E. P. T. **Metodologia de estimação de parâmetros de sistemas dinâmicos não-lineares com aplicação em geradores síncronos**. 2009. Tese (Doutorado) — Universidade de São Paulo, 2009.

CHOI, K. et al. Using the stator current ripple model for real-time estimation of full parameters of a permanent magnet synchronous motor. **IEEE Access**, IEEE, v. 7, p. 33369–33379, 2019.

ERLICH, I. et al. Determination of dynamic wind farm equivalents using heuristic optimization. In: IEEE. **2012 IEEE Power and Energy Society General Meeting**. [S.l.], 2012. p. 1–8.

ERLICH, I.; VENAYAGAMOORTHY, G. K.; WORAWAT, N. A mean-variance optimization algorithm. In: IEEE. **IEEE Congress on Evolutionary Computation**. [S.l.], 2010. p. 1–6.

FARIAS, E. R. et al. Online parameter estimation of a transient induction generator model based on the hybrid method. **IEEE Transactions on Energy Conversion**, IEEE, v. 33, n. 3, p. 1529–1538, 2018.

GOMES, G. J.; CARI, E. P. Parameter estimation of wind power plant equivalent model through a hybrid method. In: **Congresso Brasileiro de Automática-CBA**. [S.l.: s.n.], 2020. v. 2, n. 1.

GOMES, G. J. N. **Development of Software for Parameter Estimation of Wind Power Plant Equivalent**. 2020. Tese (Doutorado) — Universidade de São Paulo, 2020.

GONZÁLEZ-CAGIGAL, M.; ROSENDO-MACÍAS, J.; GÓMEZ-EXPÓSITO, A. Parameter estimation of fully regulated synchronous generators using unscented kalman filters. **Electric power systems research**, Elsevier, v. 168, p. 210–217, 2019.

GUNEN, M. A. et al. Camera calibration by using weighted differential evolution algorithm: a comparative study with abc, pso, cobide, de, cs, gwo, tlbo, mvmo, foa, lshade, zhang and bouguet. **Neural Computing and Applications**, Springer, v. 32, n. 23, p. 17681–17701, 2020.

HEYDT, G. T. et al. Estimation of synchronous generator parameters from online measurements. **Power Systems Engineering Research Center, Final Project Report PSERC Publication**, p. 05–36, 2005.

IEE. Ieee guide for test procedures for synchronous machines including acceptance and performance testing and parameter determination for dynamic analysis. **IEEE Std 115-2019 (Revision of IEEE Std 115-2009)**, p. 1–246, 2020.

IEEE. Synchronous machine stability model, an update to ieee std 1110-2002 data translation technique. In: IEEE. **2018 IEEE Power & Energy Society General Meeting (PESGM)**. [S.l.], 2018. p. 1–5.

KIMBARK, E. W. **Power system stability**. [S.l.]: John Wiley & Sons, 1995. v. 1.

KOOSHKBAGHI, M.; MARQUEZ, H. J.; XU, W. Event-triggered approach to dynamic state estimation of a synchronous machine using cubature kalman filter. **IEEE Transactions on Control Systems Technology**, IEEE, v. 28, n. 5, p. 2013–2020, 2019.

KOSTEREV N. D.; TAYLOR, C. M. W. Model validation for the august 10, 1996 esc system outage. **Power Systems, IEEE Transactions on Energy Conversion**, v. 14, p. 965–980, 1999.

KUNDUR, P. **Power system stability and control**. [S.l.]: McGraw-Hill New York, 1994. v. 7.

LANDGRAF, G. T. **Um análise de identificabilidade estrutural e prática aplicada ao modelo do gerador síncrono para estimação de parâmetros**. 2022. Tese (Doutorado) — Universidade de São Paulo, 2022.

LANDGRAF, T. G. **Modelagem e estimação de parâmetros de geradores síncronos via análise de sensibilidade de trajetória**. 2014. Dissertação (Mestrado) — Universidade de São Paulo, 2014.

LANDGRAF, T. G.; CARI, E. P.; ALBERTO, L. F. An analysis of structural and practical identifiability applied to a transient generator model. **Electric Power Systems Research**, v. 206, p. 107817, 2022. ISSN 0378-7796. Disponível em: <https://www.sciencedirect.com/science/article/pii/S0378779622000475>.

- LAVERTY, D. M. et al. The openpmu platform for open-source phasor measurements. **IEEE Transactions on Instrumentation and Measurement**, IEEE, v. 62, n. 4, p. 701–709, 2013.
- MICEV, M. et al. Field current waveform-based method for estimation of synchronous generator parameters using adaptive black widow optimization algorithm. **IEEE Access**, IEEE, v. 8, p. 207537–207550, 2020.
- PARK, R. H. Two-reaction theory of synchronous machines generalized method of analysis-part i. **Transactions of the American Institute of Electrical Engineers**, v. 48, n. 3, p. 716–727, 1929.
- RUEDA, J. L.; ERLICH, I. Hybrid single parent-offspring mvmo for solving cec2018 computationally expensive problems. In: **2018 IEEE Congress on Evolutionary Computation (CEC)**. [S.l.: s.n.], 2018. p. 1–8.
- SAUER, P.; PAI, M. Power system dynamics and control. **Printice Hall, Upper Saddle River, New Jersey**, v. 758, 1998.
- ZAKER, B. et al. Simultaneous parameter identification of synchronous generator and excitation system using online measurements. **IEEE Transactions on Smart Grid**, IEEE, v. 7, n. 3, p. 1230–1238, 2015.
- ZHU, Z.-Q.; LIANG, D.; LIU, K. Online parameter estimation for permanent magnet synchronous machines: An overview. **Ieee Access**, IEEE, v. 9, p. 59059–59084, 2021.
- ZIMMER, V.; DECKER, I.; SILVA, A. e. A robust approach for the identification of synchronous machine parameters and dynamic states based on pmu data. **Electric Power Systems Research**, Elsevier, v. 165, p. 167–178, 2018.

Annex

ANNEX A – GENERAL MODEL OF THE SYNCHRONOUS GENERATOR

A.1 General Model of the Machine

The triphasic synchronous machine can be of two types, cylindrical pole machines, and salient pole machines, it is composed of a field winding (f_d), which generates a magnetic field principal for the machine which is known as an excitation magnetic field. Consequently, the field winding generates a rotational movement driven by the turbine coupled on its axis as well as a sinusoidal voltage that is induced in three stator windings (“a”, “b”, “c”), called armature winding. Where the frequency of this voltage is determined by the angular velocity and number of magnetic poles in the stator. Besides the field and armature windings, there are short-circuited windings called damper windings which dampen oscillations in a transient regimen thus the stability characteristics of the synchronous machine improve (KUNDUR, 1994), (LANDGRAF, 2022). Therefore, the synchronous machine can be represented through six windings, if the damper windings (K_d), (K_q) are considered (as can be seen in Figure 18), where these are magnetically accoupled and the k – index is used to denote an arbitrary number of windings. The magnetic accoupled depends on the angular position (θ). In this way, the concatenated flow with each winding is a rotor’s position function (KUNDUR, 1994).

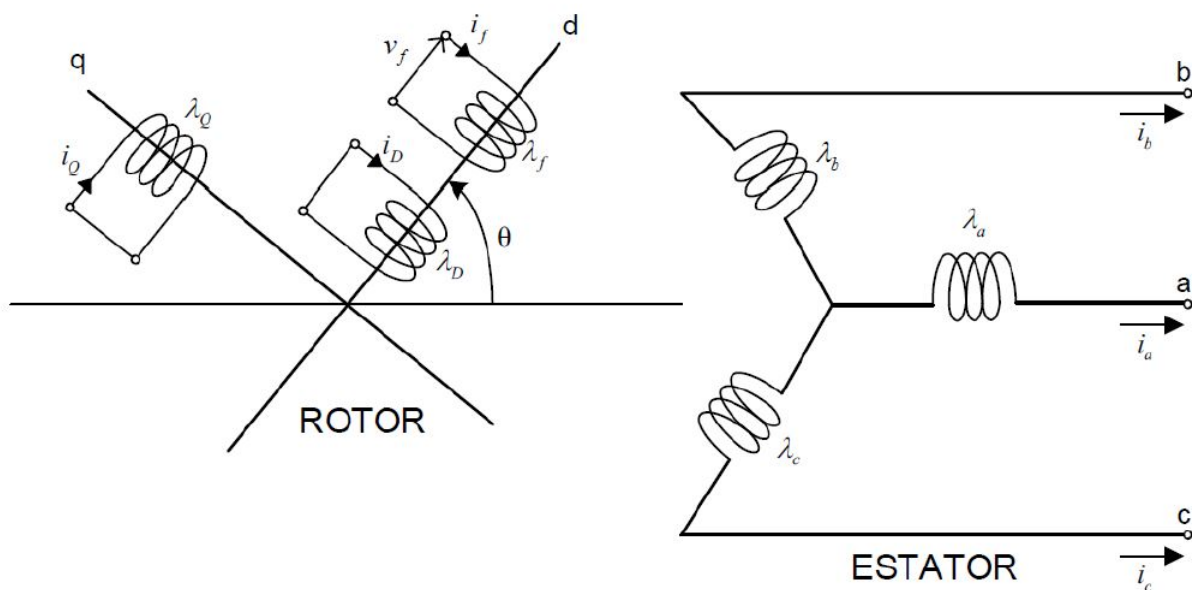


Figure 18 – Schematic representation of a synchronous machine

Source: (KUNDUR, 1994)

Figure 18 has:

- a, b, c : Stator phases windings
- i_a, i_b, i_c : Phases current “ a ”, “ b ”, and “ c ”, respectively
- ψ_a, ψ_b, ψ_c : Concatenated flow with the phase’s windings “ a ”, “ b ”, and “ c ” in the stator
- i_{fd} : Field winding current
- i_{kd}, i_{kq} : Current of the damping winding in the direct and quadrature axis, respectively
- ψ_{fd}, ψ_{kd} : Concatenated flow of damping winding of the direct and quadrature axis, respectively
- e_{fd} : Field supply voltage
- θ : Angle between direct and magnetic axis correspondent to damping of the stator of the phase “ a ”
- ω : Rotor angular velocity

In Figure 18 is shown, three windings in the stator, where each one is associated with each phase, and three windings in the rotor: a field winding, which is feeding through a continuous voltage source, and two damping windings which are short-circuited. Consequently, the field winding and two damping winding are aligned with the “d-axis” and the other is aligned with the “q-axis”.

When is applied the electromagnetic induction law (Faraday’s law) in the windings of a synchronous machine, the instantaneous terminal voltage of any of these circuits can be described by:

$$v = \pm R_i \pm \frac{d\psi}{dt} \quad (\text{A.1})$$

Where:

- R : Winding’s resistance
- i : Current
- ψ : Concatenated flow of damping

The definition of the signs (+) or (–) of the equation A.1 is dependent on the state of the machine (Generator or Motor) and the direction of the current in the winding.

Consequently, considering the machine as a generator is obtained the next equations¹:

$$v_a = -R_s i_a + \dot{\psi}_a \quad (\text{A.2})$$

$$v_b = -R_s i_b + \dot{\psi}_b \quad (\text{A.3})$$

$$v_c = -R_s i_c + \dot{\psi}_c \quad (\text{A.4})$$

Where:

- v_a, v_b, v_c : Instantaneous terminal voltages of the phases “a”, “b”, and “c” of the stator, respectively
- R_s : Winding resistance of the stator
- i_a, i_b, i_c : Instant terminal currents of the phases “a”, “b”, and “c” of the stator, respectively.

The concatenated flows (ψ) can be obtained through the next equations:

$$\psi_a = -L_{aa}i_a - L_{ab}i_b - L_{ac}i_c + L_{afd}i_{fd} + L_{akd}i_{kd} + L_{akq}i_{kq} \quad (\text{A.5})$$

$$\psi_b = -L_{ab}i_a - L_{bb}i_b - L_{bc}i_c + L_{bfd}i_{fd} + L_{bkd}i_{kd} + L_{bkq}i_{kq} \quad (\text{A.6})$$

$$\psi_c = -L_{ac}i_a - L_{cb}i_b - L_{cc}i_c + L_{cfd}i_{fd} + L_{ckd}i_{kd} + L_{ckq}i_{kq} \quad (\text{A.7})$$

Where:

- L_{aa}, L_{bb}, L_{cc} : Own inductances of the phases “a”, “b”, and “c” of the stator
- L_{ab}, L_{ac}, L_{bc} : Mutual inductances between phases “a”, “b”, and “c” of the stator
- $L_{afd}, L_{akd}, L_{akq}$: Mutual inductances of the phase “a” of the stator with the windings of $f, d,$ and q of rotor
- $L_{bfd}, L_{bkd}, L_{bkq}$: Mutual inductances of the phase “b” of the stator with the windings of $f, d,$ and q of rotor
- $L_{cfd}, L_{ckd}, L_{ckq}$: Mutual inductances of the phase “c” of the stator with the windings of $f, d,$ and q of rotor

¹ With the purpose to simplify the terms of the derivative $\frac{d}{dt}$, will be used the notation (.) above the variables.

Further, can be obtained the equations of voltage for the rotor of the synchronous machine, correspondent with field windings (f_d), direct axis damping (k_d), and quadrature axis damping (k_q), respectively:

$$e_{fd} = \dot{\psi}_{fd} \pm R_{fd}i_{fd} \quad (\text{A.8})$$

$$0 = \dot{\psi}_{kd} \pm R_{kd}i_{kd} \quad (\text{A.9})$$

$$0 = \dot{\psi}_{kq} \pm R_{kq}i_{kq} \quad (\text{A.10})$$

Where:

- R_{fd}, R_{kd}, R_{kq} : Field resistances of damping winding
- i_{fd}, i_{kd}, i_{kq} : Field currents of damping winding
- $\psi_{fd}, \psi_{kd}, \psi_{kq}$: Concatenated flow of field winding and damping winding
- e_{fd} : Field voltage

The concatenated flow of the rotor can be obtained through the next equations:

$$\psi_{fd} = -L_{fda}i_a - L_{fdb}i_b - L_{fdc}i_c + L_{ffd}i_{fd} + L_{fkd}i_{kd} + L_{fkq}i_{kq} \quad (\text{A.11})$$

$$\psi_{kd} = -L_{kda}i_a - L_{kdb}i_b - L_{kdc}i_c + L_{kdf}i_{fd} + L_{kkd}i_{kd} + L_{kdq}i_{kq} \quad (\text{A.12})$$

$$\psi_{kq} = -L_{kqa}i_a - L_{kqb}i_b - L_{kqc}i_c + L_{kqf}i_{fd} + L_{kqd}i_{kd} + L_{kkq}i_{kq} \quad (\text{A.13})$$

Where:

- $L_{ffd}, L_{kkd}, L_{kkq}$: Own inductances of winding f_d, k_d , and k_q of the rotor
- L_{fdkd}, L_{fdkq} : Mutual inductances between the field winding and damping winding of the direct axis (k_d) and the quadrature (k_q)
- $L_{fda}, L_{kda}, L_{kqa}, L_{fdb}, L_{kdb}, L_{kqb}, L_{fdc}, L_{kdc}, L_{kqc}$: Mutual inductances between the windings f_d, k_d , and k_q of the rotor and the phases “ a ”, “ b ”, and “ c ” of the stator

In accordance, with the periodic variation of mutual inductances with the position of the angle's rotor, the windings of damping can be considered. However, the differential equations presented previously will become extremely difficult to resolve. So, some suppositions can be inferred that allow resolving these equations. Firstly, the windings of the stator will be distributed in a sinusoidal way along the air gap with the purpose to minimize all harmonics components in the flow of the air gap. Another assumption is the

stator slots do not cause a significant variation in any inductance in the rotor with the angle's variation. Finally, the last assumption is that the saturation of magnetic circuits can be neglected (KUNDUR, 1994), (ADKINS; HARLEY, 2013), (LANDGRAF; CARI; ALBERTO, 2022).

This supposition can be described:

$$\begin{aligned} L_{aa} &= L_s + L_m \cos 2(\theta) \\ L_{bb} &= L_s + L_m \cos 2(\theta - 2\pi/3) \\ L_{cc} &= L_s + L_m \cos 2(\theta + 2\pi/3) \end{aligned} \quad (\text{A.14})$$

Where $L_s > L_m$, these inductances always will be positives, varying around an average value constant L_s . Thus, the own inductances of the rotor can be described:

$$L_{ffd} = L_{fd}, L_{kkd} = L_{kdk}, L_{kkq} = L_{kkq} \quad (\text{A.15})$$

Due to inductances being neglected, all will be considered constants, in addition, can be considered independents of the position of the rotor in relation to the stator.

This supposition can be described as:

$$\begin{aligned} L_{ab} &= L_{ba} = -[M_s + L_m \cos 2(\theta + \pi/6)] \\ L_{bc} &= L_{cb} = -[M_s + L_m \cos 2(\theta - \pi/6)] \\ L_{ac} &= L_{ca} = -[M_s + L_m \cos 2(\theta - 5\pi/6)] \end{aligned} \quad (\text{A.16})$$

For the phases with the axis displaced at 120° in the space, the mutual inductances always will be negatives, varying around a mean value M_s . Where L_m is the same inductance that was considered in the own inductances and such that $M_s > L_m$.

The mutual inductances between the rotor and stator are:

$$\begin{aligned} L_{afd} &= L_{fda} = M_f \cos(\theta) \\ L_{bfd} &= L_{fdb} = M_f \cos(\theta - 2\pi/3) \\ L_{cfd} &= L_{fdc} = M_f \cos(\theta + 2\pi/3) \\ L_{akd} &= L_{kda} = M_d \cos(\theta) \\ L_{bkd} &= L_{kdb} = M_d \cos(\theta - 2\pi/3) \\ L_{ckd} &= L_{kdc} = M_d \cos(\theta + 2\pi/3) \\ L_{akq} &= L_{kqa} = M_q \sin(\theta) \\ L_{bkq} &= L_{kqb} = M_q \sin(\theta - 2\pi/3) \\ L_{ckq} &= L_{kqc} = M_q \sin(\theta + 2\pi/3) \end{aligned} \quad (\text{A.17})$$

These inductances vary with the angle (θ), in the rotation frequency of the machine. Finally, the mutual inductances of the rotor are:

$$\begin{aligned} L_{fdkd} &= L_{kdfd} = M_R \\ L_{fdkq} &= L_{kqfd} = 0 \\ L_{kdkq} &= L_{kqkd} = 0 \end{aligned} \quad (\text{A.18})$$

Despite the own and mutual inductances of the rotor being constants, the inductances presented in the equations of the stator are dependents on the angular position of the rotor. Consequently, this produces that the mathematical representation of the machine will be complex. A possible solution to bypass this problem is to establish a variable transformation that fixes the greatness of the stator in the rotor of the synchronous machine. This can be obtained through $dq0$ transformation.

A.1.1 $dq0$ transformation

Park's Transformation (PARK, 1929), introduced a set of fictitious currents, voltages, and fluxes, which become functions of real currents, voltages, and fluxes. Consequently, these were substituted in the equations of the synchronous machine (KUNDUR, 1994), as can be seen in equation (A.19):

$$T_{dq0} = \frac{2}{3} \begin{bmatrix} \cos\theta & \cos(\theta - 2\pi/3) & \cos(\theta + 2\pi/3) \\ -\sin\theta & -\sin(\theta - 2\pi/3) & -\sin(\theta + 2\pi/3) \\ 1/2 & 1/2 & 1/2 \end{bmatrix} \quad (\text{A.19})$$

Performing the transformation of the $dq0$ axes to abc phases of the stator is obtained through the inverse of equation (A.19), as can be seen in equation (A.20):

$$T_{dq0}^{-1} = \frac{2}{3} \begin{bmatrix} \cos\theta & -\sin\theta & 1 \\ \cos(\theta - 2\pi/3) & -\sin(\theta - 2\pi/3) & 1 \\ \cos(\theta + 2\pi/3) & -\sin(\theta + 2\pi/3) & 1 \end{bmatrix} \quad (\text{A.20})$$

transformation of the equation (A.19) can be applied in the equations of voltages, currents of the stator, and the equations of concatenated fluxes of the stator and rotor. However, can only be applied if the set of measurements is expressed in values per unit (KUNDUR, 1994).

Applying the transformation of the equation (A.19) to the equations (A.2)-(A.4), is obtained the next equations for the voltages in the stator with respect to the $dq0$ components:

$$v_d = -R_s i_d + \dot{\psi}_d - \omega_r \psi_q \quad (\text{A.21})$$

$$v_q = -R_s i_q + \dot{\psi}_q + \omega_r \psi_d \quad (\text{A.22})$$

$$v_0 = -R_s i_0 + \dot{\psi}_0 \quad (\text{A.23})$$

Where:

- v_d, v_q, v_0 : Voltage in the direct, quadrature axis, and the zero sequence, respectively
- ω_r : Rotor's angular velocity.

Additionally, applying the transformation of the equation (A.19) to the equations (A.5)-(A.7), are obtained the values for concatenated fluxes in the stator for the $dq0$ axis system:

$$\psi_d = -L_d i_d + M_f i_f + M_d i_d \quad (\text{A.24})$$

$$\psi_q = -L_q i_q + M_q i_q \quad (\text{A.25})$$

$$\psi_0 = -L_0 i_0 \quad (\text{A.26})$$

Where:

- ψ_d, ψ_q, ψ_0 : Concatenated fluxes for direct, quadrature axis, and for zero-sequence, respectively
- L_d, L_q, L_0 : Inductance of direct, quadrature axis, and zero sequence, respectively
- i_d, i_q, i_0 : Direct, quadrature axis current, and zero sequence current, respectively

As inductances, L_d, L_q , and $-L_0$, of equations (A.24)-(A.26), are constants and independents of the angular rotor's position. In consequence, these are expressed in function to the transformation performed (KIMBARK, 1995).

$$\begin{aligned} L_d &= \left(L_s + M_s + \frac{3}{2L_m} \right) \\ L_q &= \left(L_s + M_s - \frac{3}{2L_m} \right) \\ L_0 &= L_s = -2M_s \end{aligned} \quad (\text{A.27})$$

In addition, applying the transformation (A.19) to the equations (A.11)-(A.13) obtained the following equations for the concatenated fluxes of the rotor:

$$\psi_{fd} = \left(L_f i_f + M_R i_d - \frac{3}{2} M_f i_d \right) \quad (\text{A.28})$$

$$\psi_{kd} = \left(M_R i_f + L_d i_d - \frac{3}{2} M_f i_d \right) \quad (\text{A.29})$$

$$\psi_{kq} = L_q i_q - \frac{3}{2} M_q i_q \quad (\text{A.30})$$

Normally, the manufacturers provide enough data on the synchronous machines to determine Park's model with two circuits of the rotor in the direct and quadrature axis, (BEHNAM-GUILANI, 1980), (LANDGRAF, 2022). This model will be used as a reference model and will be determined in this text as a complete model.

A.1.2 Electric Power and torque in $dq0$

The output of instant triphasic electric power of the stator can be obtained through the sum of powers of the three phases:

$$\begin{aligned}
 P_t &= v_a i_a + v_b i_b + v_c i_c = \begin{bmatrix} v_a & v_b & v_c \end{bmatrix} \begin{bmatrix} i_a \\ i_b \\ i_c \end{bmatrix} \\
 &= \begin{bmatrix} v_d & v_q & v_0 \end{bmatrix} (T_{dq0}^{-1})^{-T} (T_{dq0}^{-1}) \begin{bmatrix} i_d \\ i_q \\ i_0 \end{bmatrix} = \begin{bmatrix} v_d & v_q & v_0 \end{bmatrix} \begin{bmatrix} \frac{3}{2} & 0 & 0 \\ 0 & \frac{3}{2} & 0 \\ 0 & 0 & 3 \end{bmatrix} \begin{bmatrix} i_d \\ i_q \\ i_0 \end{bmatrix} \\
 &= \frac{3}{2} (v_d i_d + v_q i_q + 2v_0 i_0) \tag{A.31}
 \end{aligned}$$

Considering a balanced operation, where $v_0 = i_0 = 0$, the simplified power expression is shown in equation (A.32):

$$P_t = \frac{3}{2} (v_d i_d + v_q i_q) \tag{A.32}$$

Substituting the equations (A.21)-(A.23) in (A.31) to express the voltage components in concatenated flow and current terms, the power expression can be described in the following way:

$$P_t = \frac{3}{2} \left[\underbrace{(i_d \dot{\psi}_d + i_q \dot{\psi}_q + 2i_0 \dot{\psi}_0)}_{\text{Rate of variation of magnetic energy of the armature}} - \underbrace{(\psi_d i_q - \psi_q i_d) \omega}_{\text{Power transferred across the air gap}} - \underbrace{(i_d^2 + i_q^2 + 2i_0^2) R_s}_{\text{Armature resistance loss}} \right] \tag{A.33}$$

The electric torque (T_e) is transferred through the air gap and obtained by dividing the transferred power through the air gap (power of rotational voltages) by the rotor's velocity in mechanical radians per second (ω_m):

$$\begin{aligned}
 T_e &= \frac{3}{2} (\psi_d i_q - \psi_q i_d) \frac{\omega}{\omega_m} \\
 &= \frac{3p}{2} (\psi_d i_q - \psi_q i_d) \tag{A.34}
 \end{aligned}$$

Where p is the number of poles and ω_m is represented by:

$$\omega_m = \frac{2}{p} \omega \tag{A.35}$$

The concatenated flow equations (A.24)-(A.26) and (A.28)-(A.30) associated respectively to the circuits of stator and rotor, along with the voltage equations (A.21)-(A.23) for the stator, the voltage equations (A.8)-(A.10) for the rotor and the torque equation (A.34), describe the electric dynamic performance of the machine in terms of $dq0$ components.

A.1.3 Representation of equation per unit (*p.u.*)

The above equations of voltage and concatenated fluxes, can't be used to be analyzed in EES. offers simplicity in expressing variables of the system through normalization. In the case of the synchronous machine, the use of a system per unit (*p.u.*) allows removing the constants. Therefore, the mathematical representation is reduced, as well as the equations that describe the machine will be expressed in terms of the electric equivalent circuit. The base to select the system per unit (*p.u.*) for the stator is direct. On the other hand, the rotor is required careful consideration (KUNDUR, 1994).

Consequently, the application of this system per unit (*p.u.*) in synchronous machines has the same concept applied in analyses of EES, where normally is used two base values between voltage, current, impedance, and power, while, another two values will be calculated. However, in the case of synchronous machines exists an exception for velocity or frequency. Therefore, is necessary to select a base for frequency (ω) or (f_d), or the time (t). Additionally, is necessary to calculate the bases for inductances and fluxes (KUNDUR, 1994), (ANDERSON; FOUAD, 2008).

The following expressions as voltage (v_{kd}, v_{kq}), currents (i_{kd}, i_{kq}), and fluxes (ψ_d, ψ_q), are variables of the stator because have a direct relationship with *abc* phases through Park's Transformation. Thus, the current and voltages of the stator are expressed like instantaneous values that are considered how sinusoidal functions where can be found their peak values due to their peak terms. Therefore, for the conversion of the values to system per unit (*p.u.*), the following values will be considered for the stator (KUNDUR, 1994), (ANDERSON; FOUAD, 2008):

- a) Peak value of the nominal voltage of line to neutral ($\sqrt{2}V_{LN}$).
- b) Peak value of the nominal current of the line ($\sqrt{2}I_L$).
- c) Nominal frequency (H_z).

The base values for the other magnitudes of the stator are generated through three options shown in Table 19, and Table 20. The time (t) is in seconds to analyze the stability in EES. Consequently, the time constants will be expressed in seconds.

| Symbol | Description | Definition | Unit |
|----------------------------------|----------------|---|---------|
| Principal base magnitudes | | | |
| v_{sbase} | Base Voltage | Peak value of nominal voltage of line-neutral, $\sqrt{2}V_{LN}$ | V(peak) |
| i_{sbase} | Base Current | Peak value of nominal Current, $\sqrt{2}I_L$ | A(peak) |
| f_s | Base Frequency | Nominal Frequency, H_z | |
| n_p | | Poles number | |

Table 19 – Principal bases of magnitudes of the stator

| Symbol | Description | Definition | Unit |
|--------------------------------|--------------------------|--|------------|
| Derived base magnitudes | | | |
| V_{sbase} | Base Voltage (RMS) | Arbitrary selection but normally nominal voltage (RMS) of line-neutral, V_{LN} | V (RMS) |
| I_{sbase} | Base Current (RMS) | Arbitrary selection but normally nominal nominal current RMS of line, I_L | A (RMS) |
| S_{base} | Base Power (three phase) | $S_{base} = 3V_{sbase}I_{sbase} = 3\frac{v_{sbase}}{\sqrt{2}}\frac{i_{sbase}}{\sqrt{2}} = \frac{3}{2}v_{sbase}i_{sbase}$ | VA |
| ω_{base} | Electric Velocity Base | $\omega_{base} = \omega_s = 2_{base}$, where ω_s is the synchronous velocity | rad.elec/s |
| ω_{mbase} | Mechanical Velocity Base | $\omega_{mbase} = \omega_{base}(\frac{2}{p})$ is the synchronous velocity | rad.mec/s |
| Z_{sbase} | Impedance Base | $Z_{sbase} = \frac{v_{sbase}}{i_{sbase}} = \frac{V_{sbase}}{I_{sbase}}$ | Ω |
| L_{sbase} | Inductance Base | $L_{sbase} = \frac{Z_{sbase}}{\omega_{sbase}}$ | H |
| ψ_{sbase} | Flow base | $\psi_{sbase} = L_{sbase}i_{sbase} = \frac{v_{sbase}}{\omega_{sbase}}$ | V_s |
| T_{sbase} | Torque base | $T_{sbase} = \frac{S_{base}}{\omega_{mbase}} = \frac{3}{2}(=\frac{p}{2})\psi_{sbase}i_{sbase}$ | Nm |

Table 20 – Derived bases of magnitudes of the stator

Tables 19 and 20 show that the base power is equal to triphasic nominal power and the voltage and current bases values are multiplied by a factor ($\frac{3}{2}$). This can be explained due to transformation (A.19) is used, because it is not orthogonal ($T_{dq0}^-1 \neq T_{dq0}^T$), as can be seen in (A.19) and (A.20). In this way, the transformation is not invariant in power and the factor ($\frac{3}{2}$) is used to balance the power. On the other hand, when the voltage (V_{sbase}) and current (I_{sbase}) RMS values are used, base power is reached, i.e., at rated triphasic power². Furthermore, through a proper choice of the system per unit for the rotor, the factor ($\frac{3}{2}$) that multiplied the inductances in the flow equation of the rotor in (A.28)-(A.30) is discarded. The detailed development of this approach can be found in (KUNDUR, 1994). Therefore, the base values of the rotor in the reciprocal system per unit are chosen in the way that all base power equals for both stator and rotor. Accordingly, the base values of the rotor are defined in Table 21.

² A different coefficients choice of T_{dq0} matrix is used in other texts, where ($T_{dq0}^-1 = T_{dq0}^T$), therefore the transformation will be orthogonal (power invariant).

| Symbol | Description | Definition | Unit |
|--------------|--|--|----------|
| i_{fdbase} | Field base current | $i_{fdbase} = \frac{L_{ad}}{L_{afd}} i_{sbase}$ | A |
| i_{kdbase} | Base current of the damping winding of axis-d | $i_{kdbase} = \frac{L_{ad}}{L_{akd}} i_{sbase}$ | A |
| i_{kqbase} | Base current of the damping winding of axis-q | $i_{kqbase} = \frac{L_{ad}}{L_{akq}} i_{sbase}$ | A |
| e_{fdbase} | Field base voltage | $e_{fdbase} = \frac{S_{base}}{i_{fdbase}}$ | V |
| Z_{fdbase} | Field base impedance | $Z_{fdbase} = \frac{e_{fdbase}}{i_{fdbase}} = \frac{S_{base}}{i_{fdbase}^2}$ | Ω |
| Z_{kdbase} | Base impedance of damping winding of the d-axis | $Z_{kdbase} = \frac{S_{base}}{i_{kdbase}^2}$ | Ω |
| Z_{kqbase} | Base impedance of damping winding of the q-axis | $Z_{kqbase} = \frac{S_{base}}{i_{kqbase}^2}$ | Ω |
| L_{fdbase} | Field base inductance | $L_{fdbase} = \frac{Z_{fdbase}}{\omega_{base}}$ | H |
| L_{kdbase} | Base inductance of damping winding of the d-axis | $L_{kdbase} = \frac{Z_{kdbase}}{\omega_{base}}$ | H |
| L_{kqbase} | Base inductance of damping winding of the d-axis | $L_{kqbase} = \frac{Z_{kqbase}}{\omega_{base}}$ | H |

Table 21 – Base magnitudes of the rotor

This bases choice is known as $L_{ad} - base$ reciprocal system per unit:

- The mutual inductances per unit between different windings must be reciprocal
- All mutual inductances between stator and rotor circuits in each axis (d,q) are defined to be equaled in p.u. to the inductances L_{ad} , and L_{aq} , respectively

Therefore, adopting the aforementioned conditions is obtained:

$$L_{afd} = L_{fda} = L_{akd} = L_{kda} = L_{ad} \quad (\text{A.36})$$

$$L_{akq} = L_{kqa} = L_{aq} \quad (\text{A.37})$$

$$L_{kd} = L_{kdf} \quad (\text{A.38})$$

Consequently, equivalent models of electric circuits can be obtained.

A.1.4 General equations of generator model in the reciprocal system per unit

The following equations are considered two damping circuits in the q-axis and the terms $1q$ and $2q$ are used instead of kq to identify them. Just a damping circuit of the d-axis is considered and identified with the term $1d$. Both magnitudes are represented in the system per unit, except the time, which is expressed in seconds. Additionally, capital letters of the variables of the stator $V_d, V_q, V_0, I_d, I_q, I_0$ are used instead of $v_d, v_q, v_0, i_d, i_q, i_0$, respectively.

Stator voltage equations per unit, are represented by:

$$\frac{1}{\omega_s} \dot{\psi}_d = R_s I_d + \frac{\omega}{\omega_s} \psi_q + V_d \quad (\text{A.39})$$

$$\frac{1}{\omega_s} \dot{\psi}_q = R_s I_q - \frac{\omega}{\omega_s} \psi_d + V_q \quad (\text{A.40})$$

$$\frac{1}{\omega_s} \dot{\psi}_0 = R_s I_0 + V_0 \quad (\text{A.41})$$

Rotor voltage equations per unit, are represented by:

$$\frac{1}{\omega_s} \dot{\psi}_{fd} = e_{fd} - R_{fd} i_{fd} \quad (\text{A.42})$$

$$\frac{1}{\omega_s} \dot{\psi}_{1d} = -R_{1d} i_{1d} \quad (\text{A.43})$$

$$\frac{1}{\omega_s} \dot{\psi}_{1q} = -R_{1q} i_{1q} \quad (\text{A.44})$$

$$\frac{1}{\omega_s} \dot{\psi}_{2q} = -R_{2q} i_{2q} \quad (\text{A.45})$$

Consequently, the stator concatenated flow per unit is represented by:

$$\psi_d = -(L_{ad} + L_l) I_d + L_{ad} i_{fd} + L_{ad} i_{1d} \quad (\text{A.46})$$

$$\psi_q = -(L_{aq} + L_l) I_q + L_{aq} i_{1q} + L_{aq} i_{2q} \quad (\text{A.47})$$

$$\psi_0 = -L_0 I_0 \quad (\text{A.48})$$

Rotor concatenated flow equations per unit, are represented by:

$$\psi_{fd} = L_{ffd} i_{fd} + L_{f1d} i_{1d} - L_{ad} I_d \quad (\text{A.49})$$

$$\psi_{1d} = L_{f1d} i_{fd} + L_{11d} i_{1d} - L_{ad} I_d \quad (\text{A.50})$$

$$\psi_{1q} = L_{11q} i_{1q} + L_{aq} i_{2q} - L_{aq} I_q \quad (\text{A.51})$$

$$\psi_{2q} = L_{aq} i_{1q} + L_{22q} i_{2q} - L_{aq} I_q \quad (\text{A.52})$$

The electromagnetic torque of air gap per unit is represented by:

$$T_e = \psi_d I_q - \psi_q I_d \quad (\text{A.53})$$

In equations, (A.51) and (A.52) was assumed that the mutual inductance per unit L_{12q} is equal to L_{aq} because in the q-axis the field winding is not represented and the damping windings represent the global effects in this axis (KUNDUR, 1994). In this way, all stator circuits of the rotor in the q-axis concatenate a single flow represented by L_{aq} .

A.1.5 Phasor relations

This section will make an analysis of variable dimensioning. Considering a voltages balanced set per unit (KUNDUR, 1994), described by:

$$v_a = \sqrt{2}V_t \cos(\omega_s t + \theta_{vs}) \quad (\text{A.54})$$

$$v_b = \sqrt{2}V_t \cos(\omega_s t - \frac{2\pi}{3} + \theta_{vs}) \quad (\text{A.55})$$

$$v_c = \sqrt{2}V_t \cos(\omega_s t + \frac{2\pi}{3} + \theta_{vs}) \quad (\text{A.56})$$

Where:

- θ : Angular synchronous frequency
- θ_{vs} : Angle phase of v_a
- V_t : RMS value per unit of phase voltage

Using the transformation (A.19) in the equations (A.54)-(A.56):

$$V_d = \left(\frac{\sqrt{2}V_t V_{sbase}}{V_{sbase}} \right) \cos(\omega_s t + \theta_{vs} - \theta) \quad (\text{A.57})$$

$$V_q = \left(\frac{\sqrt{2}V_t V_{sbase}}{V_{sbase}} \right) \sin(\omega_s t + \theta_{vs} - \theta) \quad (\text{A.58})$$

$$V_0 = 0 \quad (\text{A.59})$$

With the definitions of Tables 19 and 20 about V_{sbase} , and v_{sbase} is obtained:

$$\frac{\sqrt{2}V_t V_{sbase}}{v_{sbase}} = \frac{\sqrt{2}V_t V_{sbase}}{\sqrt{2}V_{sbase}} = V_t \quad (\text{A.60})$$

Resulting in:

$$V_d = V_t \cos(\omega_s t + \omega_{vs} - \omega) \quad (\text{A.61})$$

$$V_q = V_t \sin(\omega_s t + \omega_{vs} - \omega) \quad (\text{A.62})$$

The angle's rotor (θ) where axis-d is ahead of phase a (Figure 18) is represented by:

$$\theta = \omega t \quad (\text{A.63})$$

Denoting (δ) is the angle's rotor where the q-axis is ahead of the phase and in relation to a synchronous reference:

$$\delta = \theta - \omega_s t \pm \frac{\pi}{2} \quad (\text{A.64})$$

Isolating (θ) of A.64 and substituting A.61 in A.62 is obtained:

$$\begin{bmatrix} V_d \\ V_q \end{bmatrix} = V_t \begin{bmatrix} \cos(\theta_{vs} - \delta + \frac{\pi}{2}) \\ \sin(\theta_{vs} - \delta + \frac{\pi}{2}) \end{bmatrix} = V_t \begin{bmatrix} -\sin(\theta_{vs} - \delta) \\ \cos(\theta_{vs} - \delta) \end{bmatrix} = V_t \begin{bmatrix} \sin(\delta - \theta_{vs}) \\ \cos(\theta_{vs} - \delta) \end{bmatrix} \quad (\text{A.65})$$

Denoting (β) as angular difference between δ and θ_{vs} :

$$\beta = (\delta - \theta_{vs}) \quad (\text{A.66})$$

Where (β) is known as the load angle

Substituting (A.66) in (A.65), the equations (A.61) and (A.62) are converted in:

$$V_d = V_t \sin(\beta) \quad (\text{A.67})$$

$$V_q = V_t \cos(\beta) \quad (\text{A.68})$$

Where V_d and V_q are components of the RMS phasor per unit of the terminal voltage of the armature phase (KUNDUR, 1994).

In the same way, $dq0$ components of the armature terminal current (I_t) can be described as phasors. If ϕ is the power factor angle is obtained:

$$I_d = I_t \sin(\beta + \phi) \quad (\text{A.69})$$

$$I_q = I_t \cos(\beta + \phi) \quad (\text{A.70})$$

Figure 19 is shown the referential frames of the synchronous generator components dq and the grid $I_m - R_e$. How the synchronous machine was equated through variable transformation, in the dq reference that is positioned in the rotor and rotates to the rotor's velocity (ω). On the other hand, the grid equations to obtain the voltages and currents in the EES are projected in the synchronous reference ($I_m - R_e$), with the R_e axis backward at 90° to the I_m axis and rotates to synchronous velocity (ω_s).

In the stability analyses, where the solution of differential equations of the synchronous machine and algebraic equations of the grid are involved, the machine models and the grid need to be properly interconnected or in the machine reference (dq reference) or in the grid reference (synchronous reference). The necessary transformation is given by (SAUER; PAI, 1998):

$$\begin{bmatrix} V_d \\ V_q \end{bmatrix} = \begin{bmatrix} \sin\delta & -\cos\delta \\ \cos\delta & \sin\delta \end{bmatrix} = \begin{bmatrix} V_{Re} \\ V_{Im} \end{bmatrix} \quad (\text{A.71})$$

The inverse transformation is given by:

$$\begin{bmatrix} V_{Re} \\ V_{Im} \end{bmatrix} = \begin{bmatrix} \sin\delta & \cos\delta \\ -\cos\delta & \sin\delta \end{bmatrix} = \begin{bmatrix} V_d \\ V_q \end{bmatrix} \quad (\text{A.72})$$

Where $V_{Re} = V_t \cos \theta_{vs}$ and $V_{Im} = V_t \sin \theta_{vs}$, there are similar relations between current terminal components as can be seen in the following equations:

$$\begin{aligned} V_{Re}^2 + V_{Im}^2 &= V_d^2 + V_q^2 = V_t^2 \\ I_{Re}^2 + I_{Im}^2 &= I_d^2 + I_q^2 = I_t^2 \end{aligned} \quad (\text{A.73})$$

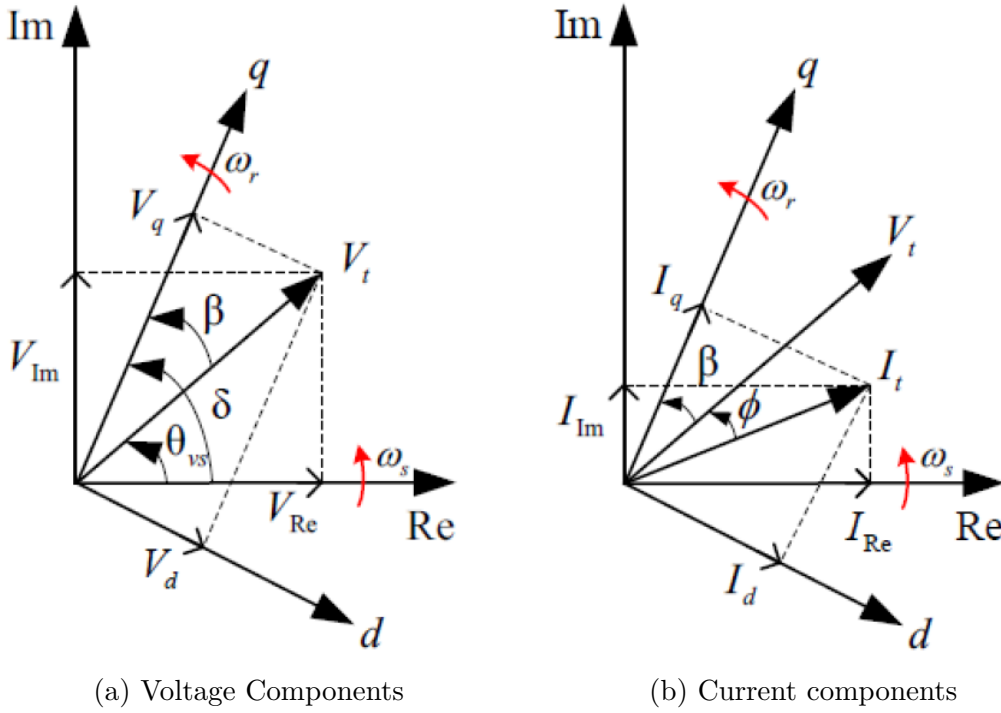


Figure 19 – Representation of $dq0$ components of terminal voltage and current armature in relation to the synchronous reference

Source: (LANDGRAF, 2022)

A.1.6 Mechanical equations

The angular position (θ) in (A.63) is measured by how stationary the reference is while (δ) in (A.64) is measured in relation to the synchronous rotation. Therefore, substituting (A.63) in (A.64), is obtained:

$$\delta = \omega t - \omega_s t + \frac{\pi}{2} \quad (\text{A.74})$$

Deriving with respect to time:

$$\frac{d\delta}{dt} = \omega - \omega_s \quad (\text{A.75})$$

Therefore, the equation of motion can be described by (KUNDUR, 1994):

$$\frac{2H}{\omega_s} \frac{d\omega}{dt} = T_m - T_e \quad (\text{A.76})$$

Where ω is the angular velocity of the rotor in rad.elec/s, ω_s is the synchronous velocity, H is the inertial constant in seconds, T_m and T_e are the mechanical and electrical torque per unit, respectively.

The equations (A.74) and (A.75) are the mechanical equations of the synchronous machine. Equation (A.76) is known as the Swing equation because it represents oscillations in the rotor's angle (δ) during the disturbances (KUNDUR, 1994).

A.1.7 Equivalent circuits

Representing the equivalent circuits is very common in the representation of the synchronous machine, though the generator performance can be described in the equations (A.39)-(A.52). Besides that, the reciprocal system per unit is used.

For system per unit, the reactance per unit can be used as the inverse of the inductances per unit. Therefore, considering inductances are obtained by multiplying the inductances by the base electric velocity (ω_s), the equivalent circuits of the d-axis and q-axis can be obtained using the flow equations for rotor and stator circuits considering their respective axis³:

- d-axis

$$\psi_d = -(X_{ad} + X_l)I_d + X_{ad}i_{fd} + X_{ad}i_{f1d} \quad (\text{A.77})$$

$$\psi_{fd} = -(X_{ffd} + i_{fd}) + X_{fd1}i_{1d} - X_{ad}I_{f1d} \quad (\text{A.78})$$

$$\psi_{1d} = -(X_{f1d} + i_{fd}) + X_{11d}i_{kd} - X_{ad}I_d \quad (\text{A.79})$$

- q-axis

$$\psi_q = -(X_{aq} + X_l)I_q + X_{aq}i_{1q} + X_{aq}i_{2q} \quad (\text{A.80})$$

$$\psi_{1q} = -(X_{11q} + i_{1d}) + X_{aq}i_{2q} - X_{aq}I_q \quad (\text{A.81})$$

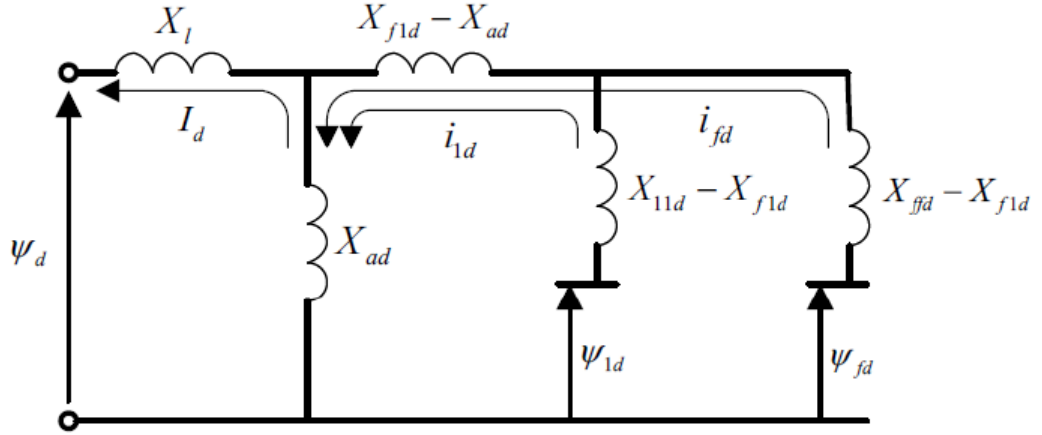
$$\psi_{2q} = -(X_{aq} + i_{1q}) + X_{22q}i_{2q} - X_{ad}I_q \quad (\text{A.82})$$

Where:

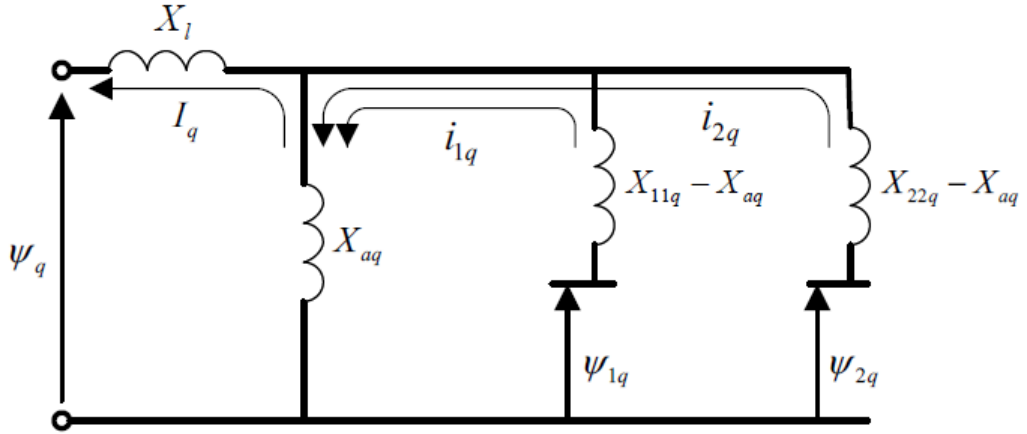
- X_l, X_{ad}, X_{aq} : Stator dispersion reactance, the mutual reactance of the d-axis, the mutual reactance of q-axis
- $X_{ffd}, X_{11d}, X_{f1q}$: Own reactance of field circuit, own reactance of damping circuit 1d, and mutual reactance between field and damping circuit 1q
- X_{11q}, X_{22q} : Own reactance of damping circuit 1q, own reactance of damping circuit 2q

³ Considering a balanced operation, zero sequence can be despised.

Figure 20a shows the equivalent circuit of d-axis using the equations (A.77)-(A.79), while Figure 20b uses the equations (A.80)-(A.82) for the equivalent circuit of q-axis.



(a) d-axis



(b) q-axis

Figure 20 – Equivalent circuits of d-axis and q-axis in relation with the flows and currents

Source: (LANDGRAF, 2022)

According to Figure 20 is introduced for the rotor circuit the following dispersion reactances per unit:

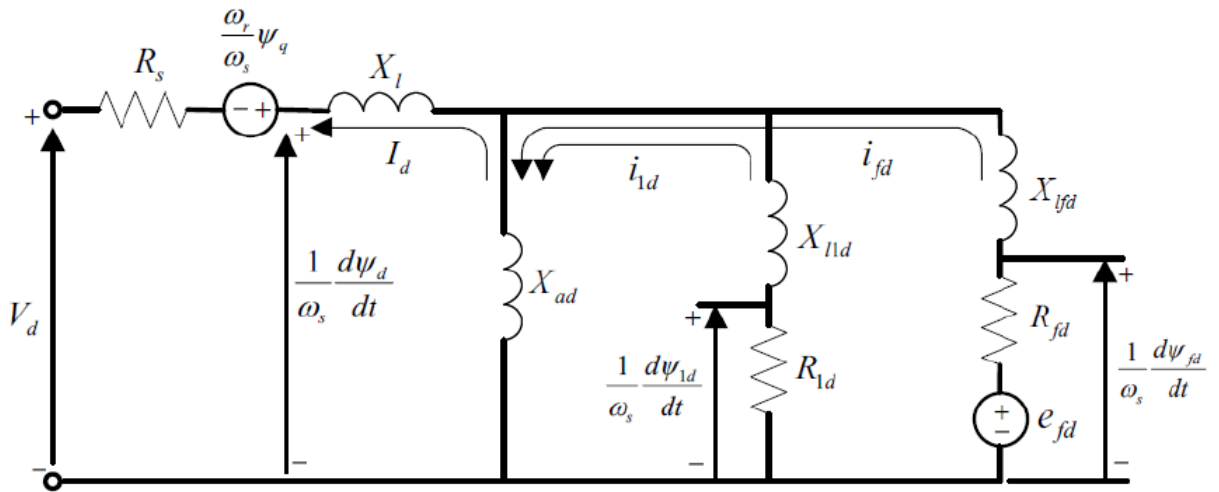
$$X_{1fd} = X_{ffd} - X_{ad} \quad (\text{A.83})$$

$$X_{l1d} = X_{11d} - X_{ad} \quad (\text{A.84})$$

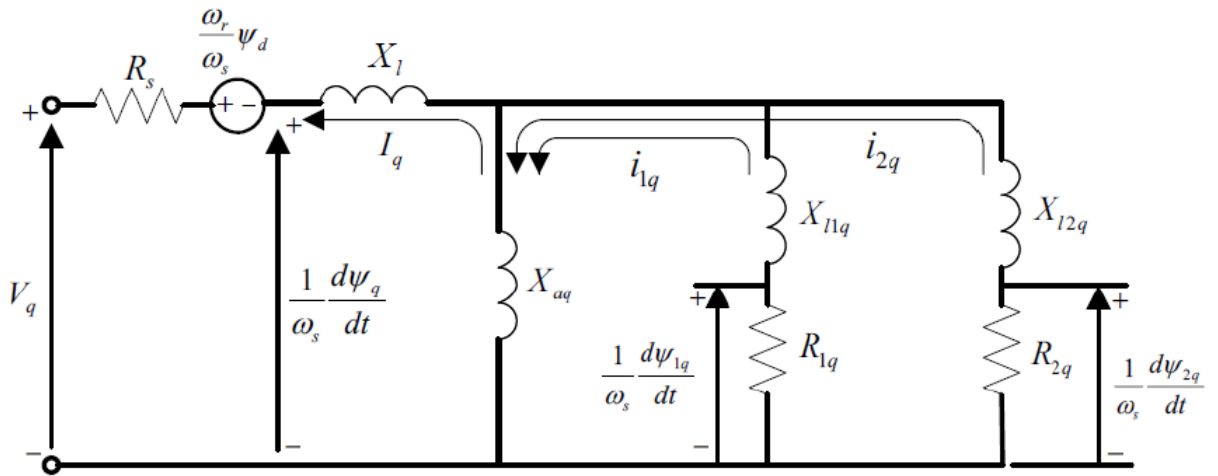
$$X_{l1q} = X_{11q} - X_{aq} \quad (\text{A.85})$$

$$X_{l2q} = X_{22q} - X_{aq} \quad (\text{A.86})$$

In addition, the mutual reactances X_{f1d} and X_{ad} are considered equals, this makes all mutual inductances in the d-axis equal (KUNDUR, 1994). In this way, series reactances $X_{f1d} - X_{ad}$ represented in the equivalent circuit of the d-axis (Figure 20) disappear. Therefore, the equivalent circuits with complete characteristics considering the voltages equations (A.39)-(A.45) are shown in Figure 21.



(a) Equivalent circuit of d-axis



(b) Equivalent circuit of q-axis

Figure 21 – Complete equivalent circuits of d-axis and q-axis

Source: (LANDGRAF, 2022)

A.1.8 Synchronous machine parameters per unit

The synchronous machine parameters correspond to the reactances and resistances of rotor and stator circuits (Figure 21). They are known as fundamental or basic parameters of equivalent circuit elements of the d-axis and q-axis.

Although these fundamental parameters describe the complete electric characteristics of the machine, this cannot be determined directly through machine measurements. Therefore, standard parameters are defined by intermission of fundamental parameters (KUNDUR, 1994), (SAUER; PAI, 1998):

$$X_d = X_l + X_{ad} \quad (\text{A.87})$$

$$X_q = X_l + X_{aq} \quad (\text{A.88})$$

$$X'_d = X_l + \frac{1}{\frac{1}{X_{ad}} + \frac{1}{X_{lfd}}} = X_l + \frac{X_{ad}X_{lfd}}{X_{ad} + X_{lfd}} = X_d - \frac{X_{ad}^2}{X_{ffd}} \quad (\text{A.89})$$

$$X'_q = X_l + \frac{1}{\frac{1}{X_{aq}} + \frac{1}{X_{l1q}}} = X_l + \frac{X_{aq}X_{l1q}}{X_{aq} + X_{l1q}} = X_q - \frac{X_{aq}^2}{X_{11q}} \quad (\text{A.90})$$

$$X''_d = X_l + \frac{1}{\frac{1}{X_{ad}} + \frac{1}{X_{lfd}} + \frac{1}{X_{l1d}}} \quad (\text{A.91})$$

$$X''_q = X_l + \frac{1}{\frac{1}{X_{aq}} + \frac{1}{X_{l1q}} + \frac{1}{X_{l2q}}} \quad (\text{A.92})$$

$$T'_{d0} = \frac{X_{ad} + X_{lfd}}{\omega_s R_{fd}} = \frac{X_{ffd}}{\omega_s R_{fd}} \quad (\text{A.93})$$

$$T'_{q0} = \frac{X_{aq} + X_{l1q}}{\omega_s R_{1q}} = \frac{X_{11q}}{\omega_s R_{1q}} \quad (\text{A.94})$$

$$T''_{d0} = \frac{1}{\omega_s R_{1d}} \left(X_{l1d} + \frac{1}{\frac{1}{X_{ad}} + \frac{1}{X_{lfd}}} \right) \quad (\text{A.95})$$

$$T''_{q0} = \frac{1}{\omega_s R_{2q}} \left(X_{l2q} + \frac{1}{\frac{1}{X_{aq}} + \frac{1}{X_{l1q}}} \right) \quad (\text{A.96})$$

Where:

- X_d, X'_d, X''_d : Synchronous reactance, transient reactance, and sub-transient reactance in d-axis (p.u.)
- X_q, X'_q, X''_q : Synchronous reactance, transient reactance, and sub-transient reactance in q-axis (p.u.)
- T'_{d0}, T''_{d0} : Transient and sub-transient time constants of the open circuit of d-axis (s)
- T'_{q0}, T''_{q0} : Transient and sub-transient time constants of the open circuit of q-axis (s)

A.1.8.1 Parameters of salient pole machine

The standard parameters obtained in (A.87)-(A.96) were developed for a model with two rotor circuits in each axis⁴, it can be applied in a smooth pole machine. However, for a salient pole machine, just is necessary a damping winding in the q-axis, therefore, the rotor circuit has just one circuit in the q-axis ($2q$). The other parameters of this rotor circuit represent the sub-transient effects. The second rotor circuit ($1q$), is ignored. Consequently, the expressions for the standard parameters in the q-axis of the salient pole machine are given by:

$$X_q = X_l + X_{aq} \quad (\text{A.97})$$

$$X_q'' = X_l + \frac{X_{aq}X_{12q}}{X_{aq} + X_{12q}} \quad (\text{A.98})$$

$$T_{q0}'' = \frac{X_{aq} + X_{12q}}{\omega_s R_{2q}} = \frac{X_{22q}}{\omega_s R_{2q}} \quad (\text{A.99})$$

The transient parameters X_q' and T_q' are not applicable to this model.

For the d-axis is considered two circuits for the rotor (field winding fd and damping winding $1d$) as in the case of smooth poles machine, the expressions obtained in the equations (A.87)-(A.96) for parameters of smooth poles machine equal to salient poles machine.

A.1.9 Synchronous machine variables per unit

The variables are the following equations:

$$E_q' = \frac{X_{dd}}{X_{ffd}} \psi_{fd} = \text{Proportionalvoltage to } \psi_{fd} \quad (\text{A.100})$$

$$E_d' = -\frac{X_{aq}}{X_{11q}} \psi_{1q} = \text{Proportionalvoltage to } \psi_{1q} \quad (\text{A.101})$$

$$E_{fd} = \frac{X_{ad}}{R_{fd}} e_{fd} = \text{Proportionalvoltage to } e_{fd} \quad (\text{A.102})$$

A.1.9.1 Dynamic equations of synchronous generator

The dynamic equations of synchronous generator including mechanical and electric equations:

$$\dot{\delta} = \omega - \omega_s \quad (\text{A.103})$$

$$\frac{2H}{\omega_s} \dot{\omega} = T_m - (\psi_d I_d - \psi_q I_q) \quad (\text{A.104})$$

⁴ Two circuits in d-axis, the field winding fd and winding $1d$, and two circuits in q-axis, damping winding $1q$ and $2q$.

$$\frac{1}{\omega_s} \dot{\psi}_d = R_s I_d + \frac{\omega}{\omega_s} \psi_q + V_d \quad (\text{A.105})$$

$$\frac{1}{\omega_s} \dot{\psi}_q = R_s I_q + \frac{\omega}{\omega_s} \psi_d + V_q \quad (\text{A.106})$$

$$\frac{1}{\omega_s} \dot{\psi}_{fd} = -R_{fd} i_{fd} + e_{fd} \quad (\text{A.107})$$

$$\frac{1}{\omega_s} \dot{\psi}_{1d} = -R_{1d} i_{1d} \quad (\text{A.108})$$

$$\frac{1}{\omega_s} \dot{\psi}_{1q} = -R_{1q} i_{1q} \quad (\text{A.109})$$

$$\frac{1}{\omega_s} \dot{\psi}_{2q} = -R_{2q} i_{2q} \quad (\text{A.110})$$

Considering $X_{f1d} = X_{ad}$, the concatenated flow equations in d-axis are:

$$\psi_d = -(X_{ad} + X_l) I_d + X_{ad} i_{fd} + X_{ad} i_{1d} \quad (\text{A.111})$$

$$\psi_{fd} = X_{ffd} i_{fd} + X_{ad} i_{1d} - X_{ad} I_d \quad (\text{A.112})$$

$$\psi_{1d} = X_{ad} i_{fd} + X_{11d} i_{kd} - X_{ad} I_d \quad (\text{A.113})$$

The concatenated flows in the q-axis are:

$$\psi_q = -(X_{aq} + X_l) I_q + X_{aq} i_{1q} + X_{aq} i_{2q} \quad (\text{A.114})$$

$$\psi_{1q} = X_{11q} i_{1q} + X_{aq} i_{2q} - X_{aq} I_q \quad (\text{A.115})$$

$$\psi_{2q} = X_{aq} i_{1q} + X_{22q} i_{2q} - X_{aq} I_q \quad (\text{A.116})$$

The algebraic equations (A.111)-(A.116) can be reorganized using the parameter defined in (A.87)-(A.96) and the variables defined in (A.87)-(A.96) in the following way:

$$\psi_d = -X_d'' I_d + \frac{(X_d'' - X_l)}{(X_d' - X_l)} E_q' + \frac{(X_d' - X_d'')}{(X_d' - X_l)} \psi_{1d} \quad (\text{A.117})$$

$$i_{fd} = \frac{1}{X_{md}} [E_q' + (X_d - X_q')(I_d - i_{1d})] \quad (\text{A.118})$$

$$i_{1d} = \frac{(X_d' - X_d'')}{(X_d' - X_l)^2} [\psi_{1d} + (X_d' - X_l) I_d - E_q'] \quad (\text{A.119})$$

$$\psi_q = -X_q'' I_q - \frac{(X_q'' - X_l)}{(X_q' - X_l)} E_d' + \frac{(X_q' - X_q'')}{(X_q' - X_l)} \psi_{2q} \quad (\text{A.120})$$

$$i_{1q} = \frac{1}{X_{md}} [-E_d' + (X_q - X_q')(I_q - i_{2q})] \quad (\text{A.121})$$

$$i_{2q} = \frac{(X_q' - X_q'')}{(X_q' - X_q)^2} [\psi_{2q} + (X_q' - X_l) I_q + E_q'] \quad (\text{A.122})$$

Substituting (A.116)-(A.121) in (A.103)-(A.110), provides the following model of the generator:

$$\dot{\delta} = \omega - \omega_s \quad (\text{A.123})$$

$$\frac{2H}{\omega_s} \dot{\omega} = T_m - (\psi_d I_q - \psi_q I_d) \quad (\text{A.124})$$

$$\frac{1}{\omega_s} \dot{\psi}_d = R_s I_d + \frac{\omega}{\omega_s} \psi_q + V_d \quad (\text{A.125})$$

$$\frac{1}{\omega_s} \dot{\psi}_q = R_s I_q - \frac{\omega}{\omega_s} \psi_d + V_q \quad (\text{A.126})$$

$$T'_{d0} \dot{E}'_q = -\dot{E}'_q - (X_d - X'_d) \left[I_d - \frac{(X'_d - X''_d)}{(X'_d - X''_d)^2} (\psi_{1d} + (X'_d - X_{ls}) I_d - E'_q) \right] + E_{fd} \quad (\text{A.127})$$

$$T''_{d0} \dot{\psi}_{1d} = -\psi_{1d} + E'_q - (X'_d - X_l) I_d \quad (\text{A.128})$$

$$T'_{q0} \dot{E}'_d = -\dot{E}'_d + (X_q - X'_q) \left[I_q - \frac{(X'_q - X''_q)}{(X'_q - X''_q)^2} (\psi_{2q} + (X'_q - X_l) I_q + E'_d) \right] \quad (\text{A.129})$$

$$T''_{q0} \dot{\psi}_{2q} = -\psi_{2q} - E'_d - (X'_q - X_l) I_q \quad (\text{A.130})$$

With the following algebraic equations:

$$\psi_d = -X''_d I_d + \frac{(X''_d - X_l)}{(X'_d - X_l)} E'_q + \frac{(X'_d - X''_d)}{(X'_d - X_l)} \psi_{1d} \quad (\text{A.131})$$

$$\psi_q = -X''_q I_q + \frac{(X''_q - X_l)}{(X'_q - X_l)} E'_d + \frac{(X'_q - X''_q)}{(X'_q - X_l)} \psi_{2q} \quad (\text{A.132})$$

These equations complete the dynamic model of the synchronous generator, if the saturation of the magnetic circuit were negligence, in the same way, it will be used to obtain the simplified model.

A.1.10 Simplified Models

The use of the complete model of the synchronous generator (A.123)-(A.132) in simulations will be tedious in transient stability studies due to its elevated order. In consequence, some simplified models were developed to simplify the complexity of the model and make the analysis of more complex systems feasible.

A.1.10.1 Dynamic equations of synchronous generator

The transient model is reduced from the complete model from eighth-order to sixth-order. Therefore, stator transients are despised. This simplification is plausible because the changing voltages ($\dot{\psi}_k d, \dot{\psi}_k q$) are small in relation to rotational voltages ($\omega_r \psi_{kq}, \omega_r \psi_{kd}$). Additionally, if stator transients ($\dot{\psi}_k d, \dot{\psi}_k q$) were neglected, the resulting algebraic equations will be resolved simultaneously with the grid (SAUER; PAI, 1998), (LANDGRAF, 2022). The model obtained still has the same number of damper windings as the complex model.

The differential equations that describe this model are the following:

$$\dot{\psi}_{fd} = -R_{fd}i_{fd} + v_{fd} \quad (\text{A.133})$$

$$\dot{\psi}_{1d} = -R_{1d}i_{1d} \quad (\text{A.134})$$

$$\dot{\psi}_{1q} = -R_{1q}i_{1q} \quad (\text{A.135})$$

$$\dot{\psi}_{2q} = -R_{2q}i_{2q} \quad (\text{A.136})$$

How is possible to see the above equations, the condition $\dot{\psi}_{1q} = 0$ continues to be valid for salient poles machines. However, the equations that describe the mechanical transients were omitted for simplicity.

If the equations of the model are written in terms of variables of the stator, this will be (\dot{E}'_q, \dot{E}'_d) instead of $(\dot{\psi}_{fd}, \dot{\psi}_{1q})$. More information about this model can be obtained in (LANDGRAF, 2014), (CARI; LANDGRAF; ALBERTO, 2017). Such model is known as the Two-axis model can be described as follows:

$$\dot{\omega} = \frac{\omega_0}{2H} \left(P_m - E'_q I_q - E'_d I_d - (x_d - x'_d) I_d I_q - \frac{D}{\omega_0} \omega \right) \quad (\text{A.137})$$

$$\dot{\delta} = \omega - \omega_s \quad (\text{A.138})$$

$$\dot{E}'_q = \frac{1}{T'_{d0}} \left(E_{fd} - E'_q + (x_d - x'_d) I_d \right) \quad (\text{A.139})$$

$$\dot{E}'_d = \frac{-1}{T'_{q0}} \left(E'_d + (x_q - x'_q) I_q \right) \quad (\text{A.140})$$

$$I_d = \frac{V_t \cos(\beta) - E'_q}{x'_d} \quad (\text{A.141})$$

$$I_q = \frac{V_t \sin(\beta) + E'_d}{x'_q} \quad (\text{A.142})$$

Where:

- E'_{fd} : Proportional voltage to field voltage
- E'_d, E'_q : Transient voltage in the direct and quadrature axis, respectively
- I_d, I_q : Current in the direct and quadrature axis, respectively
- x'_d, x'_q : Transient reactance in the direct and quadrature axis
- D, H : Damping and Inertia constants
- T'_{d0}, T'_{q0} : Time transient constant of the open circuit in the direct and quadrature axis, respectively
- δ : Rotor's angle
- ω : Angular velocity

- β : Generator rotor angle of quadrature axis
- V_t : Generator rotor angle of quadrature axis

For the transient generator model, the variables are:

$$\begin{array}{ll}
 \text{Parameters:} & p = [x_d, x'_d, T'_{d0}, T'_{q0} x'_q, x'_q, E'_{d0}, E'_{q0}, H, D]^T \\
 \text{State variables:} & x = [E'_q, E'_d] \\
 \text{Algebraic variables:} & x = [E'_q, E'_d] \\
 \text{Input variables:} & u = [E_{fd}, I_q, V_t] \\
 \text{Output variables:} & y = [P_e, Q_e]
 \end{array}$$

For such model, the state (E'_d) and (E'_q) cannot be measured and the rotor's angle (δ) is very difficult to measure in the practice. Therefore, the initial conditions of the state variable E'_{d0} E'_{q0} and the rotor's angle (δ) must be considered as parameters, so the number of the parameters increases to nine, which entails a worse numerical condition. Another problem with the estimation of many parameters is the intrinsic problem where the measurement of the angular velocity (ω) and the estimation of the rotor's angle (δ) are not enough to estimate the generator rotor angle of the quadrature axis (β) with precision. In other words, the angle (β) is not observable, more information can be found in (CARI, 2009) (LANDGRAF; CARI; ALBERTO, 2022).

In equations (A.137)-(A.142), the capital letters are variables used in root mean square (RMS) values. Additionally, when $\dot{\psi}_{1q} = 0$, for salient pole machines ($x'_q = x_q$), the model is reduced. Thus, the variable $E'_d = 0$. Consequently, the transient model for the salient pole generator is like the Two-axis model with the difference that $E'_d = 0$, this model is known as the "One-axis" model.

Consequently, the original one-axis transient model of the synchronous generator will be presented in chapter 2 for didactic purposes.

In (CARI, 2009) is developed an improved transient generator model for parameter estimation purposes obtained from the traditional transient generator model (A.137)-(A.142). The advantages of the model are to diminish the number of parameters to be estimated and to use only measurements usually available in the real system. Those models will be shown in chapter 2.

ANNEX B – MVMO ALGORITHM INFORMATION

Proposed in (ERLICH; VENAYAGAMOORTHY; WORAWAT, 2010), being the first step of Figure 4, this algorithm is a population-based metaheuristic method that uses a mapping function to be able to mutate and create new generations through the mean and variance of the best population. Population evolution shares characteristics with other algorithms that also managed to evolve (GOMES; CARI, 2020). Nonetheless, these are different due to the way they induce mutations in the offspring to diversify the population. Consequently, the MVMO method updates the solution according to the best solution at each iteration.

On the other hand, since during the mutation process, the statistical data of the population are considered, the MVMO method introduces a memory shape factor, which improves the search mechanism. Therefore, the MVMO is considered a robust method because it combines the mapping function with the intelligent search technique. It also provides better performance compared to other metaheuristic methods when the population size is small (ERLICH; VENAYAGAMOORTHY; WORAWAT, 2010), (ERLICH et al., 2012).

The goal of the MVMO method is to perform good optimization, so you need to consider two very important concepts. First, exploration (global search) deals with a broad search performed through the region of interest. Second, exploitation (local search) performs the search on a small data set that is very close to the best solutions. For better understanding, the terms "gene", "individual", and "population" are referred to as "parameters", "parameter vector", and "parameter vector set" respectively.

In summary, the steps of the MVMO algorithm are as follows:

a. Initialization:

- Define limits of each parameter $p_i \in [p_i^{min}, p_i^{max}]$ based on experience.
- Definition of an individual as a parameter vector \mathbb{R}^{np} .
- Definition of a population as set of individuals $\mathbb{R}^{nk} \times \mathbb{R}^{np}$.
- Define the number of individuals (n_p).
- Generate the initial population $n_k \times n_p$.

b. Fitness assessment:

- Use one input of measured data from each set of parameters, to compute the outputs of model (3.3), determine the objective function $J(p)$ for each individual, and rank the population from the best (smallest $J(p)$) to worst (largest $J(p)$).

- If $J(p)$ of the best parameter vector (individual) is less than a tolerance ($tol_1 = 1 \times 10^{-3}$) stop, else go to the next steps.
- Normalize the parameter vector using equation (B.1):

$$p_i^{norm} = \frac{p_i - p_i^{min}}{p_i^{max} - p_i^{min}} \quad (B.1)$$

- Determine the population mean and variance as shown in Figure 22, using equations (B.2), (B.3):

$$\bar{p}_i = \frac{1}{n_k} \sum_i^n p_i(i) \quad (B.2)$$

$$v_i = \frac{1}{n_k} \sum_i^j (p_i(j) - \bar{p}_i)^2 \quad (B.3)$$

| | Individuals | p_1 (gene 1) | p_2 (gene 2) | \dots | p_{np} (gene np) | Fitness Function $J(p)$ | |
|---------------------------------|------------------|--------------------------------|-------------------|-------------|-----------------------|----------------------------|--|
| Best \updownarrow Worst | Individual 1 | Individual parent: Ind_{Par} | | | | Unnormalize parameters | |
| | Individual 2 | | | | | | |
| | ⋮ | Population | | | | | |
| | ⋮ | | | | | | |
| | Individual nk | | | | | | |
| | Mean \bar{p}_i | \bar{p}_1 | \bar{p}_2 | \bar{p}_3 | \bar{p}_{np} | - | |
| | Variance v_i | v_1 | v_2 | v_3 | v_{np} | - | |
| Factors | s_i | | | | | | |
| | d_{i0} | | | | | | |
| | d_i | | | | | | |
| | S_{r1} | | | | | | |
| | S_{i2} | | | | | | |

Figure 22 – Procedure step by step for MVMO

- Determine shape factor s_i by equation (B.4):

$$s_i = -\ln(v_i) \times f_s \quad (B.4)$$

Where f_s is a factor that defines the shape of the mapping function. Therefore, if $f_s > 1$ the precision of the estimation is improved (flat curve). However, if $f_s < 1$, the global search is performed (increase the slope of the curve). In [Erlich et al. \(2012\)](#) some spaces such as $f_s \in [0.9 - 1]$ and $f_s \in [1 - 10]$ are recommended when f_s is less than and greater than 1. A dynamic factor is obtained by equation (B.5):

$$f_s = f_s^*(1 + rand) \quad (\text{B.5})$$

Where f_s^* is given by equation (B.6):

$$f_s^* = f_{sini}^* + \left(\frac{i}{i_{fin}}\right)^2 (f_{sfin}^* - f_{sini}^*) \quad (\text{B.6})$$

Some recommended values are $f_{sini}^* \in [0, 9 - 1]$ and $f_{sfin}^* \in [1 - 3]$

- Determine factor s_{i1} and s_{i2} using the next algorithm

if $s_i \geq d_i$ then $d_i = d_i \times f_d$

else $d_i = \frac{d_i}{f_d}$

if $rand \geq 0.5$ then $s_{i1} = s_i; s_{i2} = d_i$

else $s_{i1} = d_i; s_{i2} = s_i$

Where f_d is a factor that makes d_i oscillate around s_i given by equation (B.7), as shown in Figure 23:

$$f_d = 1 + 2 \times rand \times \Delta d0 \quad (\text{B.7})$$

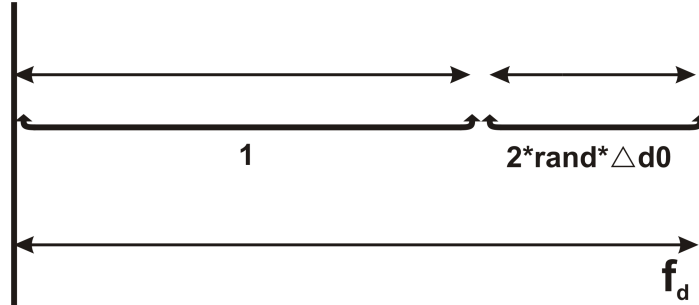


Figure 23 – Representation of the factor f_d .

A dynamic factor for $\Delta d0$ can be obtained by equation (B.8):

$$\Delta d0 = \Delta d0_{ini} + \left(\frac{i}{i_{fin}}\right)^2 (\Delta d0_{fin} - \Delta d0_{ini}) \quad (\text{B.8})$$

Initially, $di = dio$ will be updated at each iteration. The procedure is represented also in Figure 22.

c. Offspring generation

- Assign the best individual, best parameter vector, p_{best} as the parent, as shown in Figure 24.

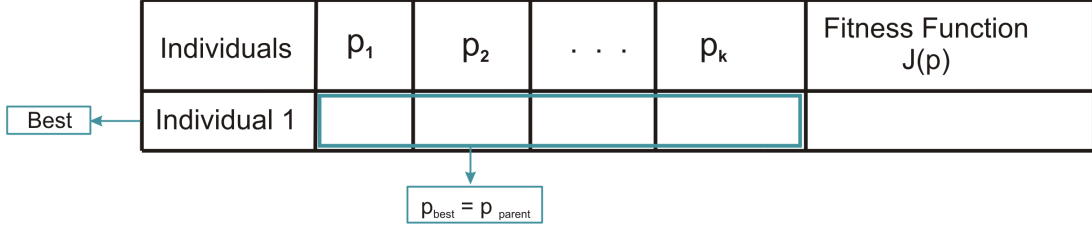


Figure 24 – Selection of the best individual.

- Select (randomly) elements of best individual p_{parent} which be altered by the mapping function, as shown in Figure 25.

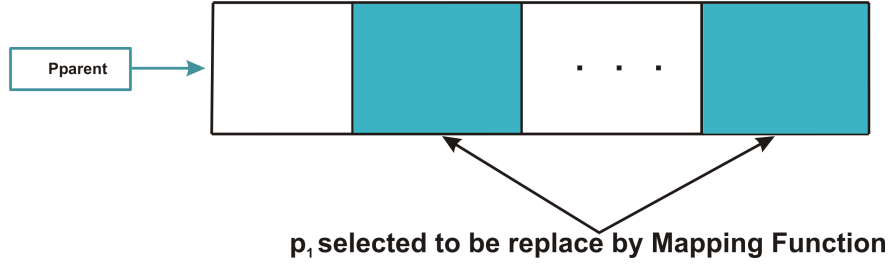


Figure 25 – Gene of the parent replaced in the mapping function.

- Using $s_{i1}, s_{i2}, \bar{p}_i$ and an aleatory number $p_i^* = rand$ in (3.2), determine new values for the n elements of p_{best} by the mapping function given by equations (B.9), (B.10).

$$p_{inew} = H_{MF}(\bar{p}_i, s_{i1}, s_{i2}, p_i^*) \quad (B.9)$$

$$p_{inew} = h(\bar{p}_i, s_{i1}, s_{i2}, p_i^*) + [1 - h(\bar{p}_i, s_{i1}, s_{i2}, 1) + h(\bar{p}_i, s_{i1}, s_{i2}, 0)] * p_i^* - h(\bar{p}_i, s_{i1}, s_{i2}, 0) \quad (B.10)$$

Where the function h is given by equation (B.11):

$$h(\bar{p}_i, s_{i1}, s_{i2}, p) = \bar{p} \cdot (1 - e^{-x \cdot s_1}) + (1 - \bar{p}) * e^{-(1-x) \cdot s_2} \quad (B.11)$$

With this approach, p_{inew} will be concentrated around the mean value, as shown in Figure 26.

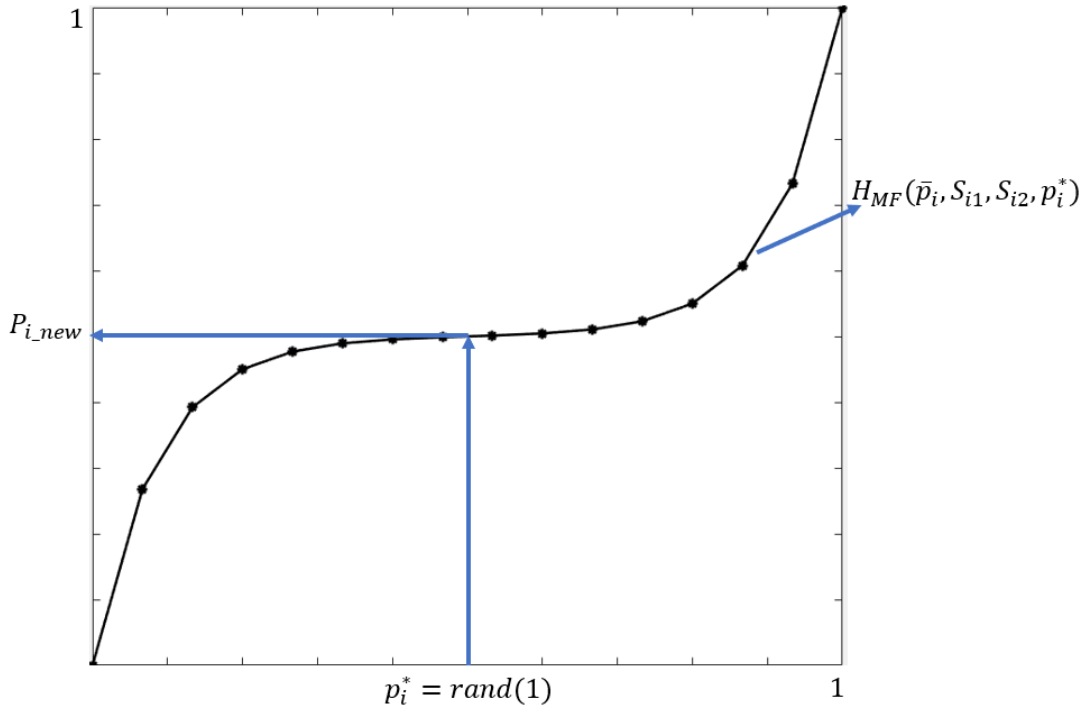


Figure 26 – Concentration around the mean value.

- For the remaining elements of p_i use the same of p_{parent} , as shown in Figure 27.
- Using the new elements, p_{new} ranked all the individuals again according to their fitness function, discarded the worst element, and then went to step b, as shown in Figure 28 and Figure 29.



Figure 27 – New individual p_{new} obtained from p_{parent} remaining elements of p_i .

| Individuals without ranked | p_1 | p_2 | ... | p_k | Fitness Function $J(p)$ |
|----------------------------|-------|-----------------------|-----|-------------|-------------------------|
| Individual 1 | | | | | |
| Individual 2 | | | | | |
| Individual 3 | | New Population | | | |
| ... | | | | | |
| Individual n_p | | | | | |
| $n_p + 1$ | | $p_{1,new}$ | ... | $p_{2,new}$ | |

p_{parent}

 New individual

Figure 28 – Population with the new individual without ranked.


| | Individuals ranked | p_1 | p_2 | . . . | p_k | Fitness Function $J(p)$ |
|--------------------|----------------------|--|--------------|-------|--------------|-------------------------|
| Worst ↑ Best | Individual 1 | | | | | |
| | Individual 2 | | | | | |
| | Individual $n_p + 1$ | | p_{1_new} | . . . | p_{2_new} | |
| | Individual 3 | | | | | |
| | Individual 4 | | | | | |
| | Individual n_p |  | | | | |

Figure 29 – Population ranked from the best to the worst individuals including the new individual and discarding the worst one.

- Repeat all procedures until $J(p)$ is less than a predefined tolerance.

According to (GOMES; CARI, 2020), the main advantage of the MVMO method is its good performance using small populations, restricted search regions, and avoiding divergence. However, a common problem with heuristic methods is the time they take when it is close to the local minimum. To reduce the total convergence time, the method will change after a few MVMO generations to a non-linear TSM, which is very efficient when the initial vector is close to the solution. More information about MVMO algorithm can be found in (ERLICH; VENAYAGAMOORTHY; WORAWAT, 2010).